An Investigation on the Geometric Effects of a Vertical-Downward Elbow on Two-Phase Flow

Philip Graybill
Grove City College
Mechanical Engineering

Andrew Hardison
Robert Morris University
Mechanical Engineering

Advisor: Dr. Seungjin Kim
Penn State University
Mechanical and Nuclear Engineering

July 30, 2015

Generously sponsored by the
Toshiba-Westinghouse Fellows Program

This presentation investigates the geometric effects of a vertical-downward elbow on two-phase flow.

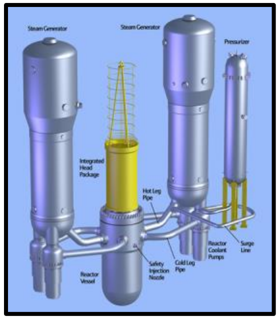

Background

Objective

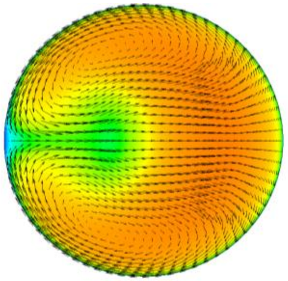

Single-Phase Flow CFD Modeling

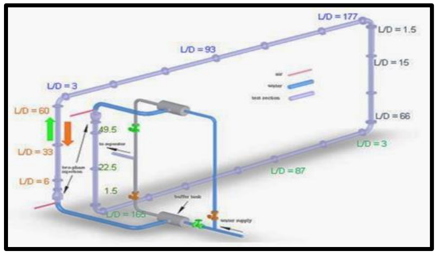

Two-Phase Flow Investigation

Researching geometric effects on two-phase flow can improve the safety of thermal-hydraulic reactor systems.

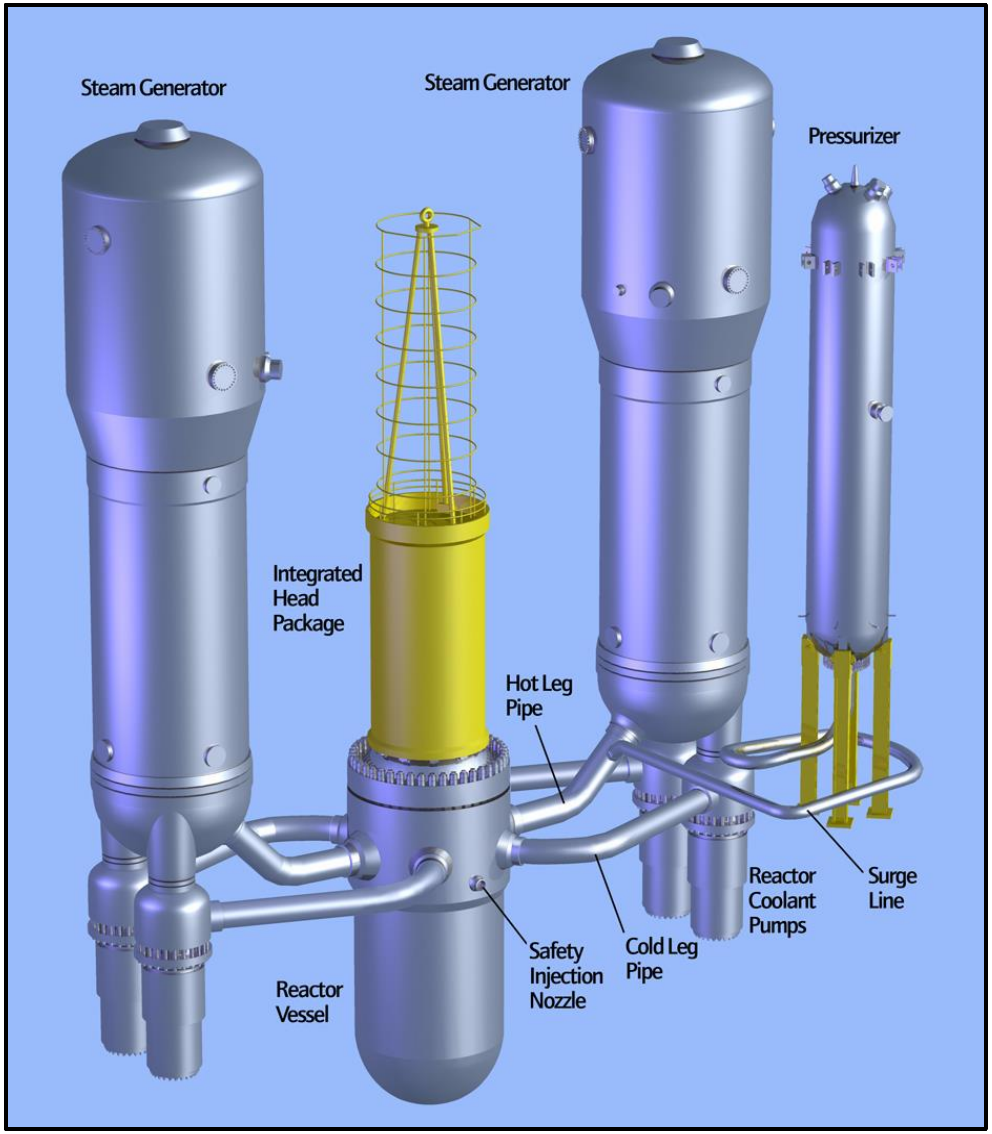

Geometry and pipe orientation dramatically affect two-phase flow.

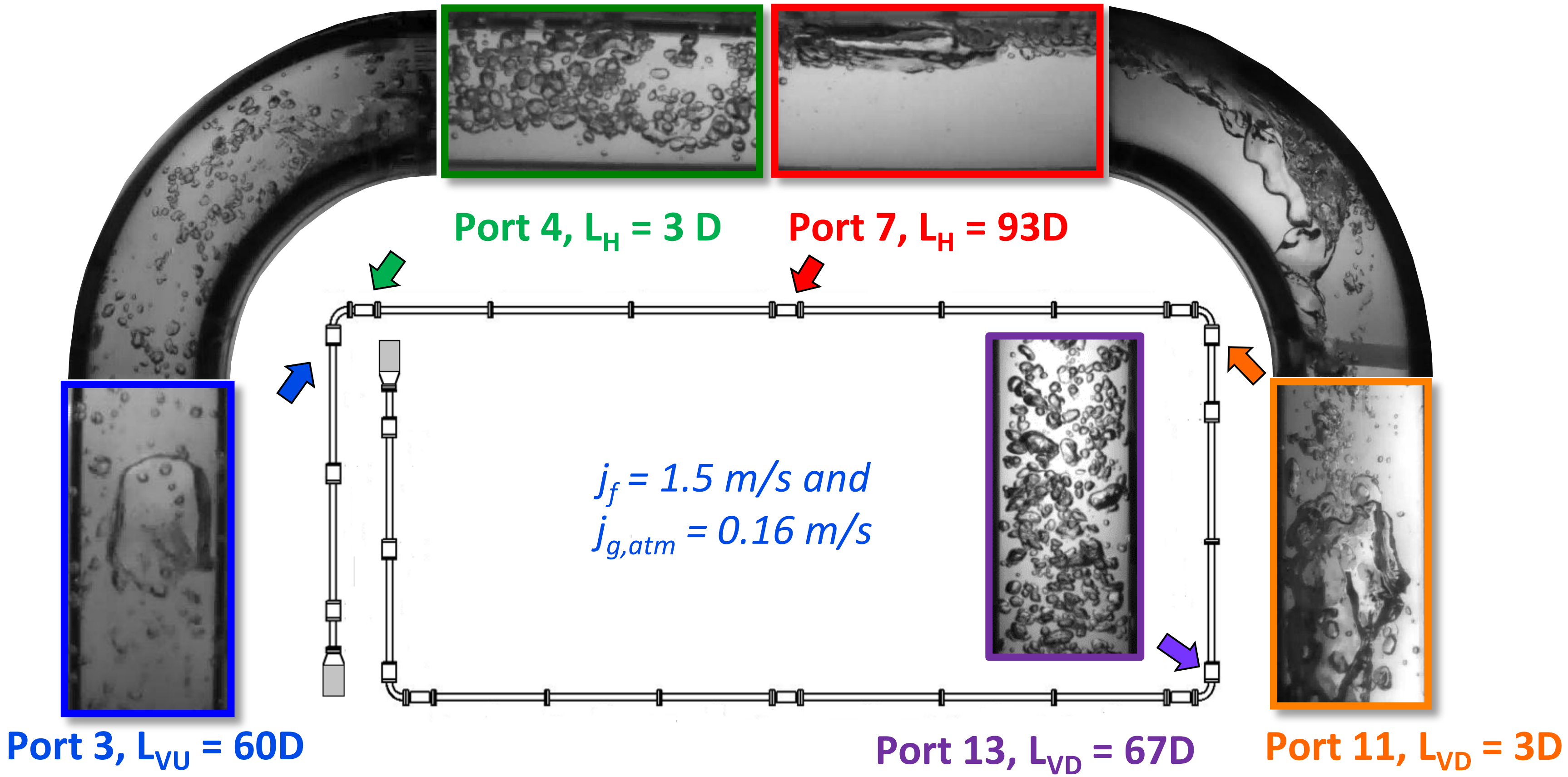

The experimental facility at Penn State enables data collection for a vertical-downward elbow.

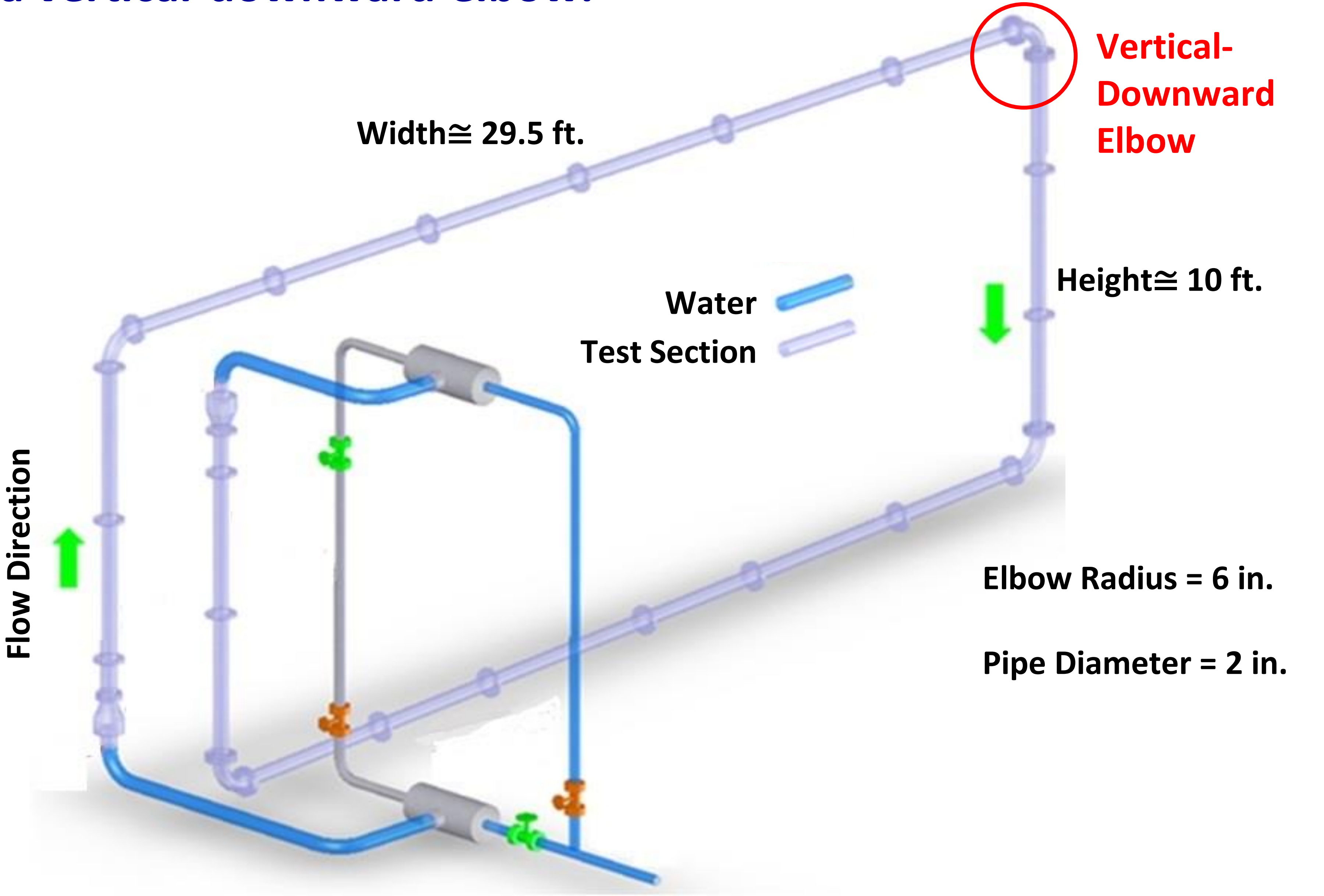

The experimental facility at Penn State enables data collection for a vertical-downward elbow.

Combinatorial Test Facility

Vertical-Downward Elbow

The objective of this research is to investigate the impacts of a vertical-downward elbow.

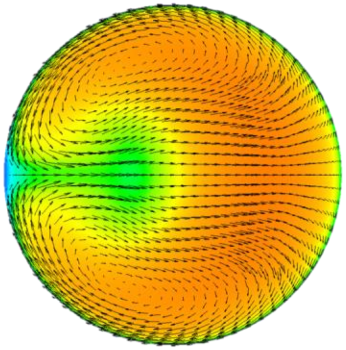

Single-phase CFD analysis

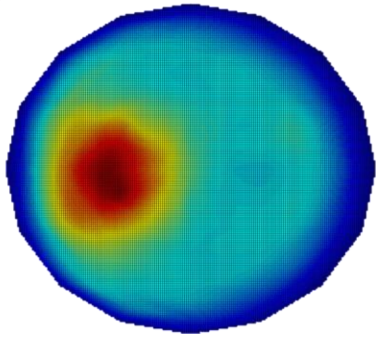

Establish Database

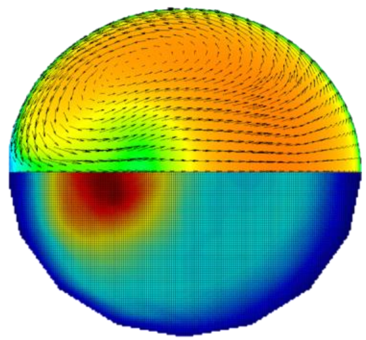

Comparison

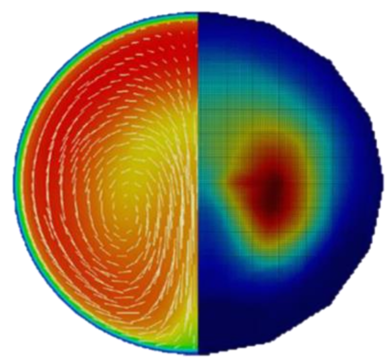

Previous Studies Comparison

Single-phase flow in the facility was modeled with CFD to better understand the general elbow effects.

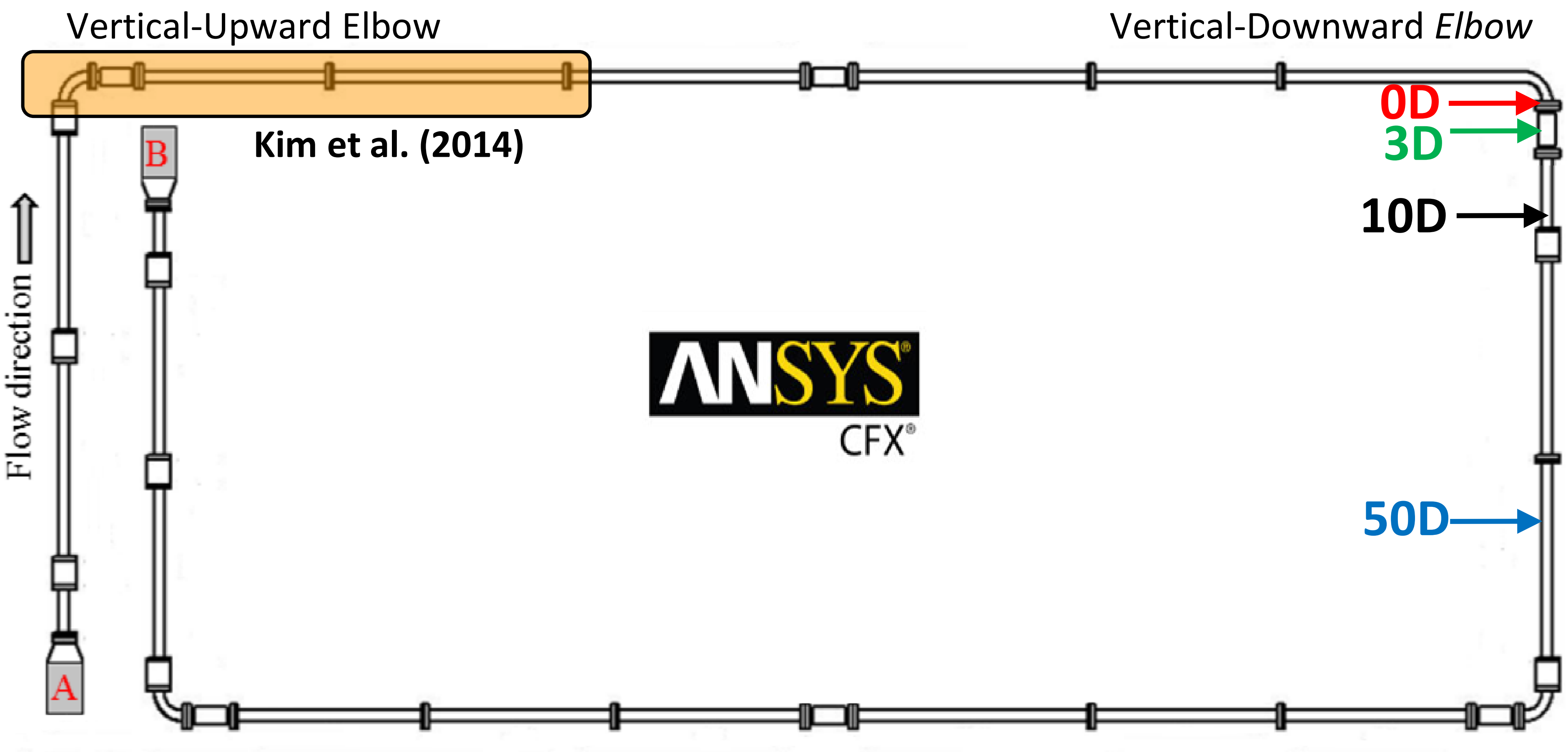

A turbulent secondary flow structure is created after the vertical-downard elbow.

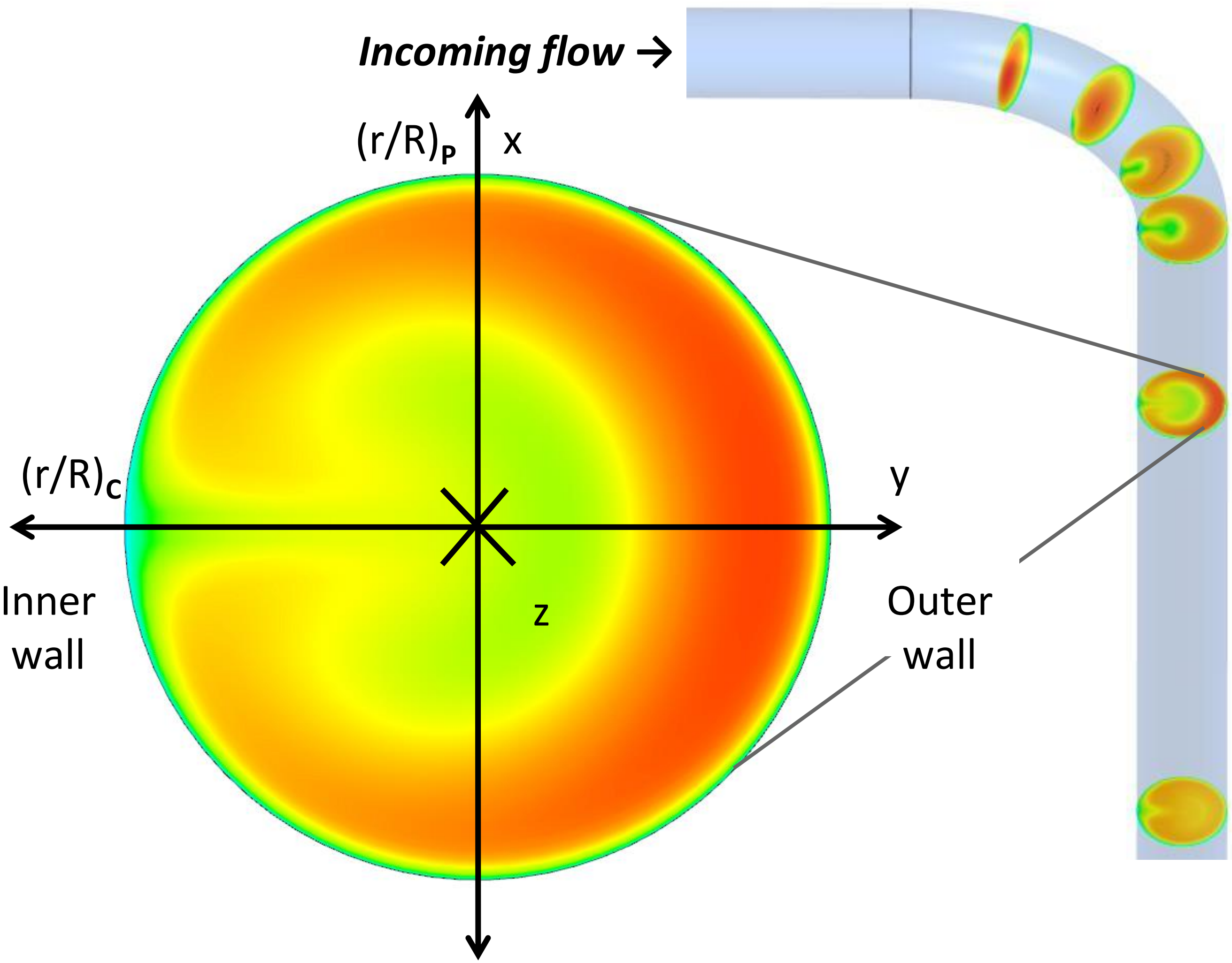

A secondary flow structure is created after the vertical-downard elbow.

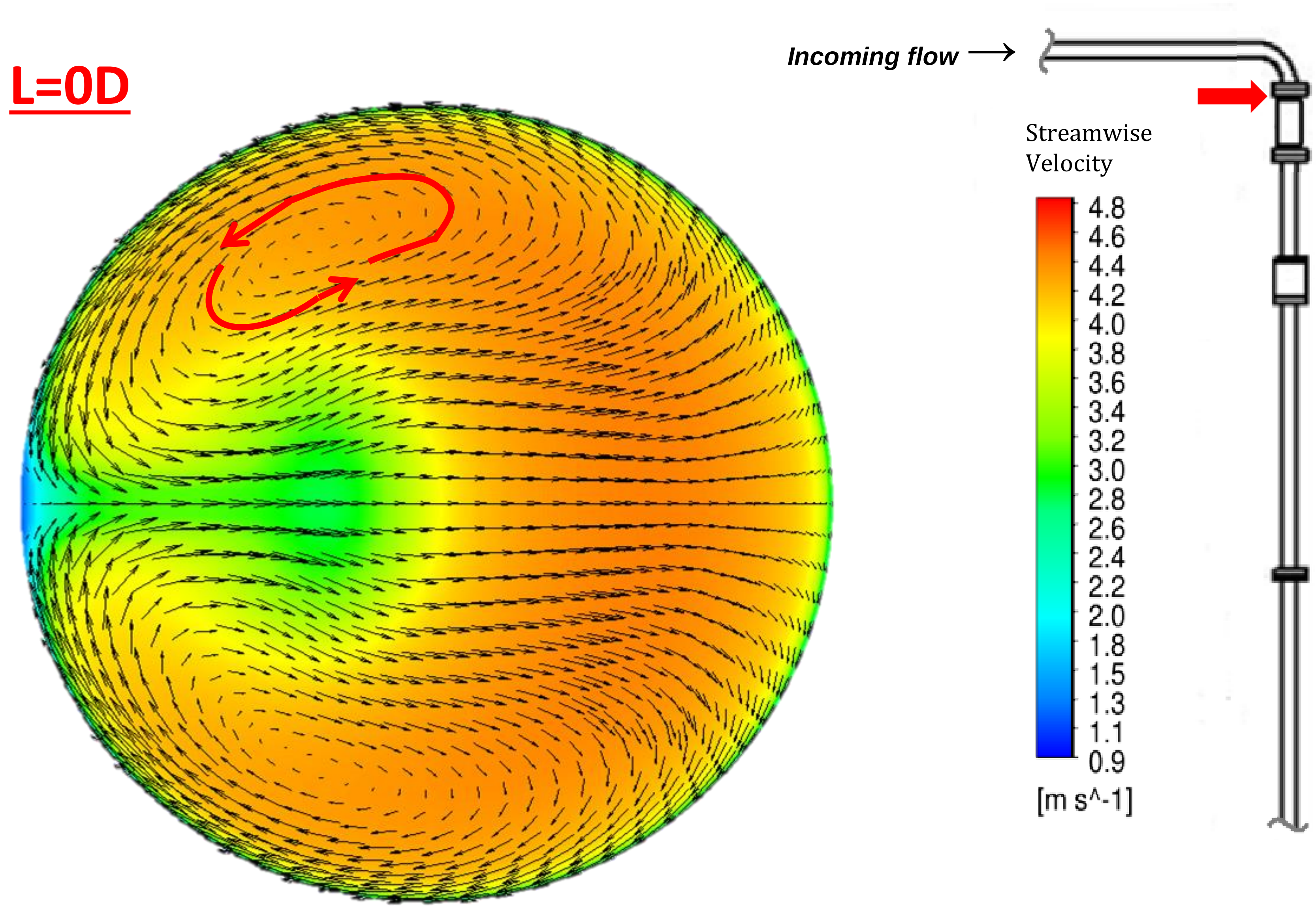

A secondary flow structure is created after the vertical-downard elbow.

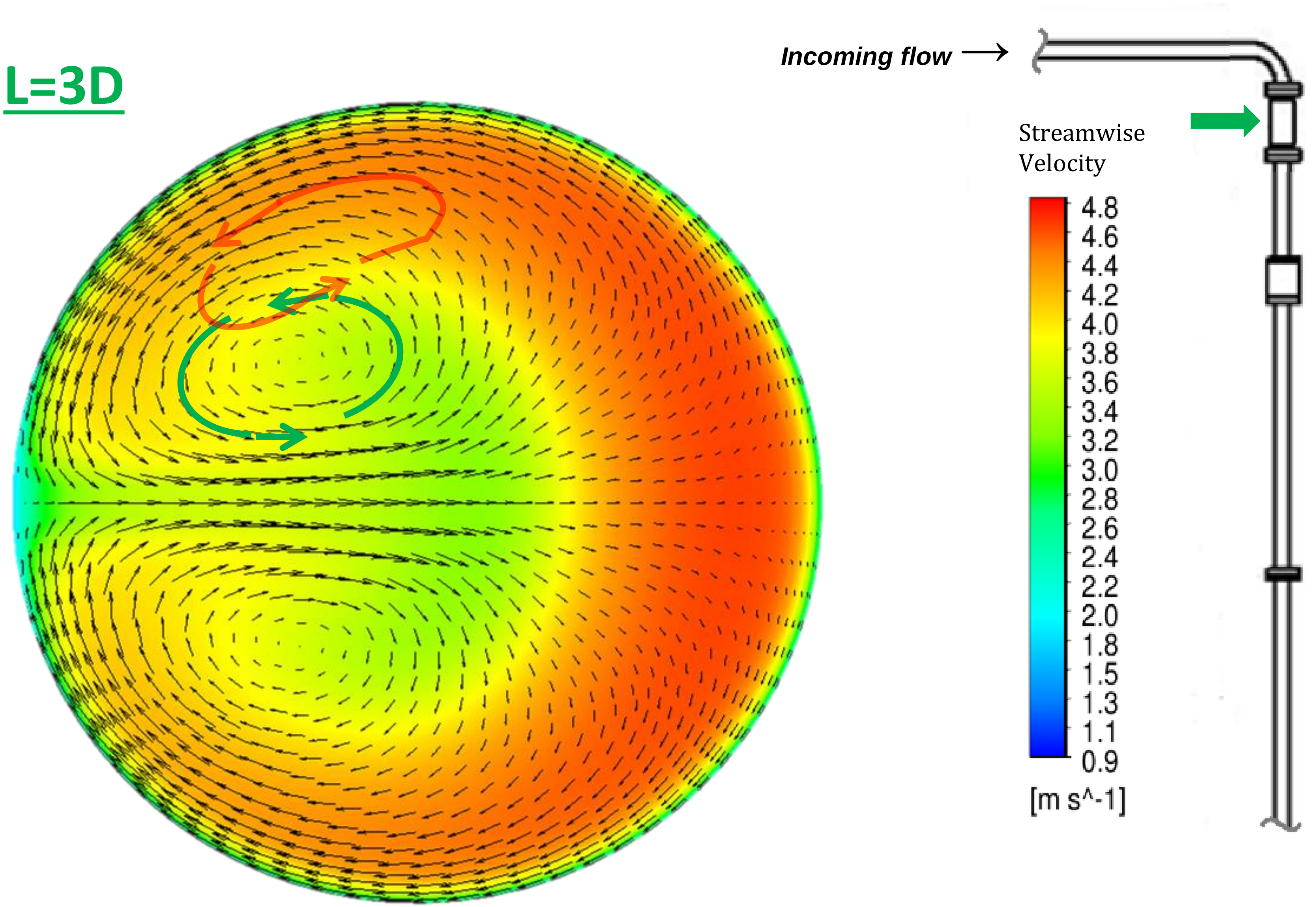

A secondary flow structure is created after the vertical-downard elbow.

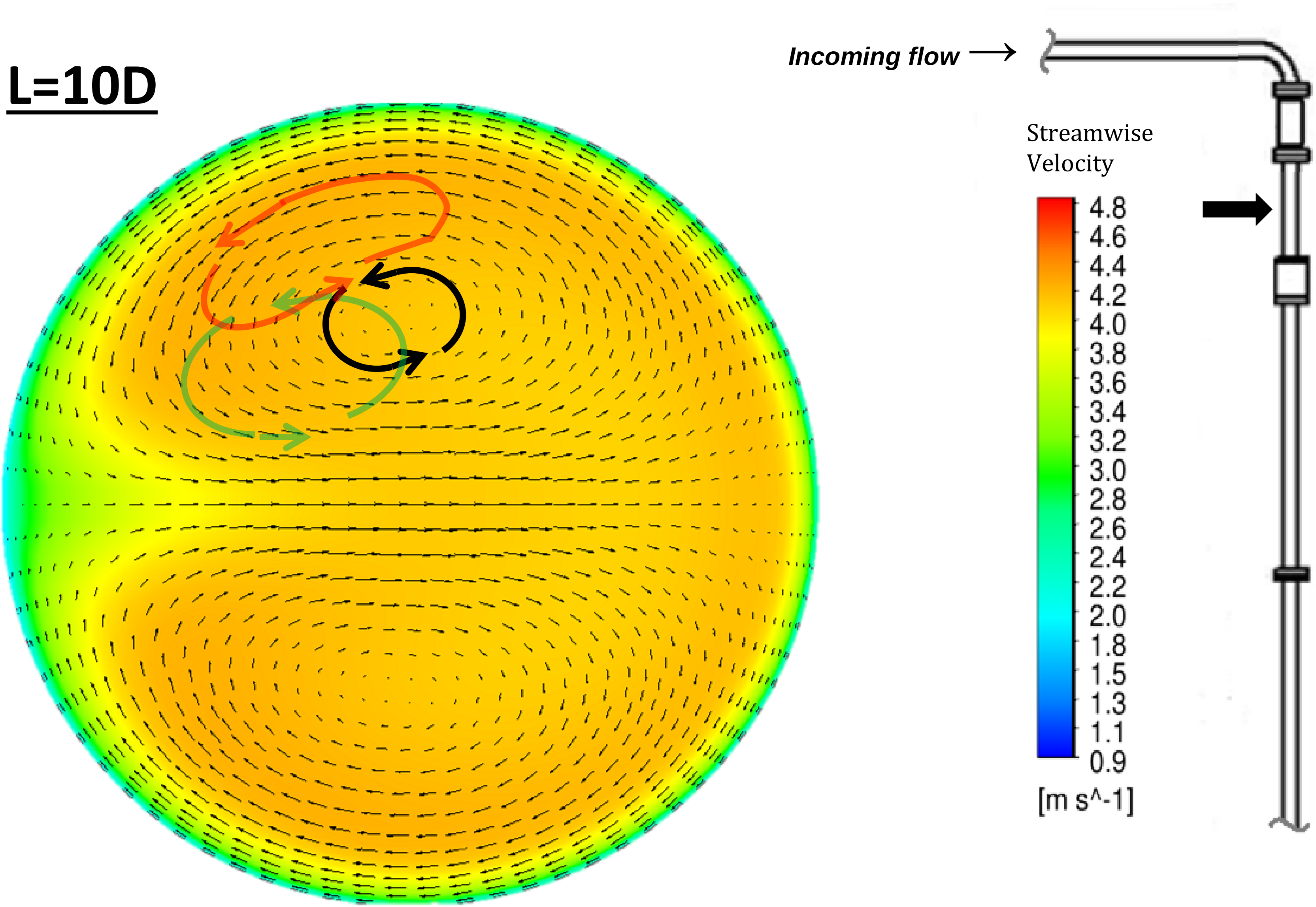

A secondary flow structure is created after the vertical-downard elbow.

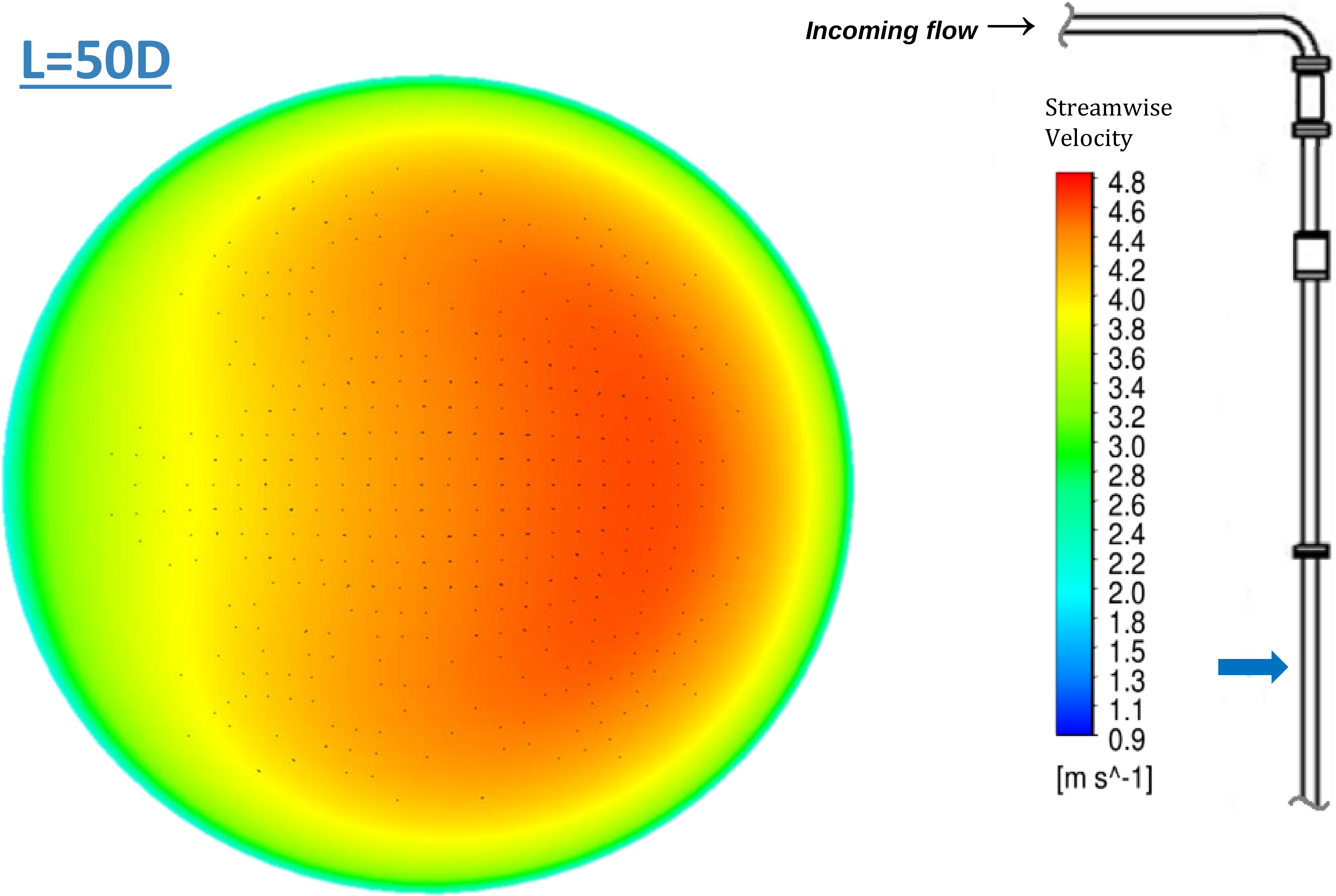

A secondary flow structure is created after the vertical-downard elbow.

Progression Sequence

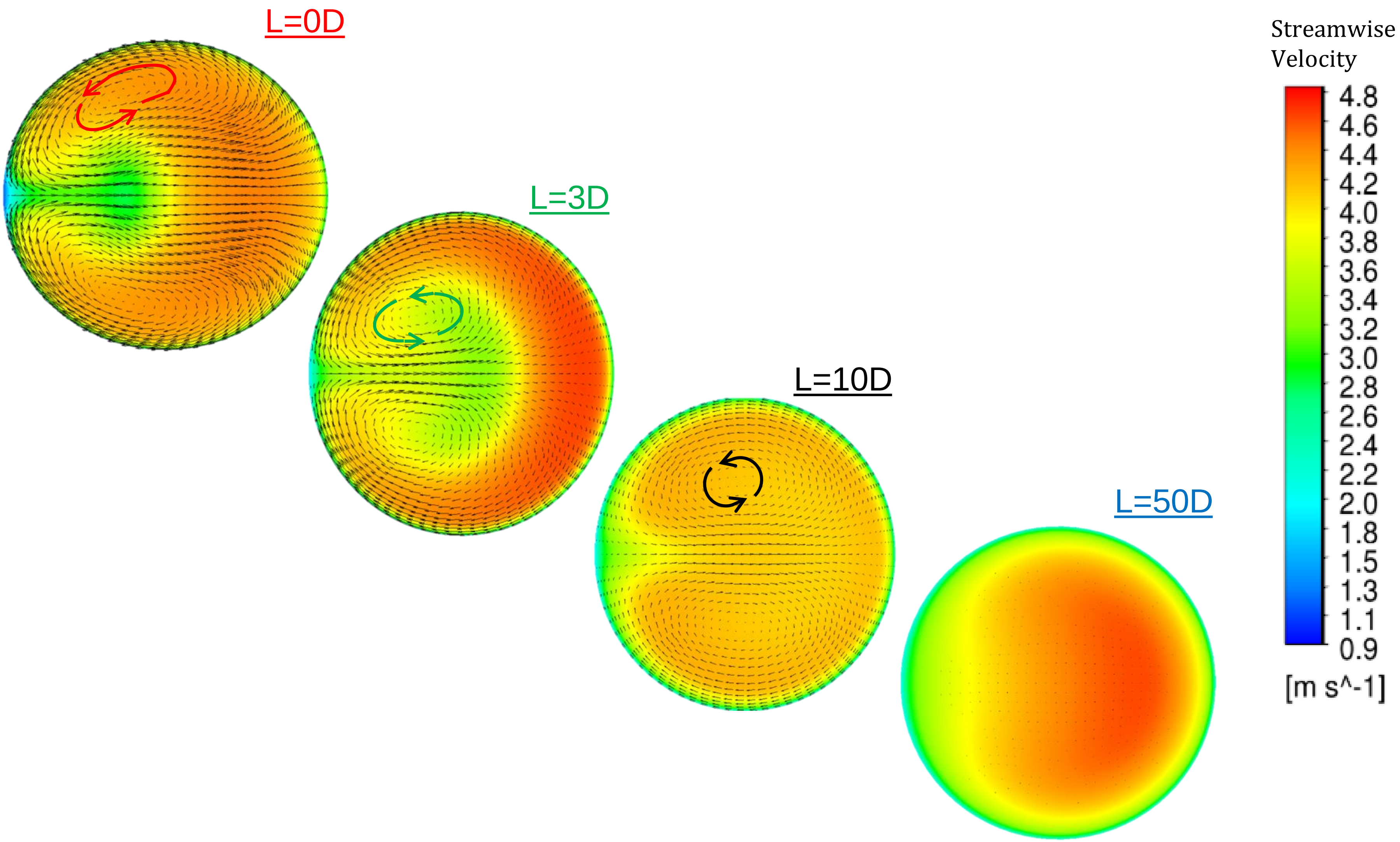

A four-sensor conductivity probe collects local data as it moves across the pipe with a specialized measurement port.

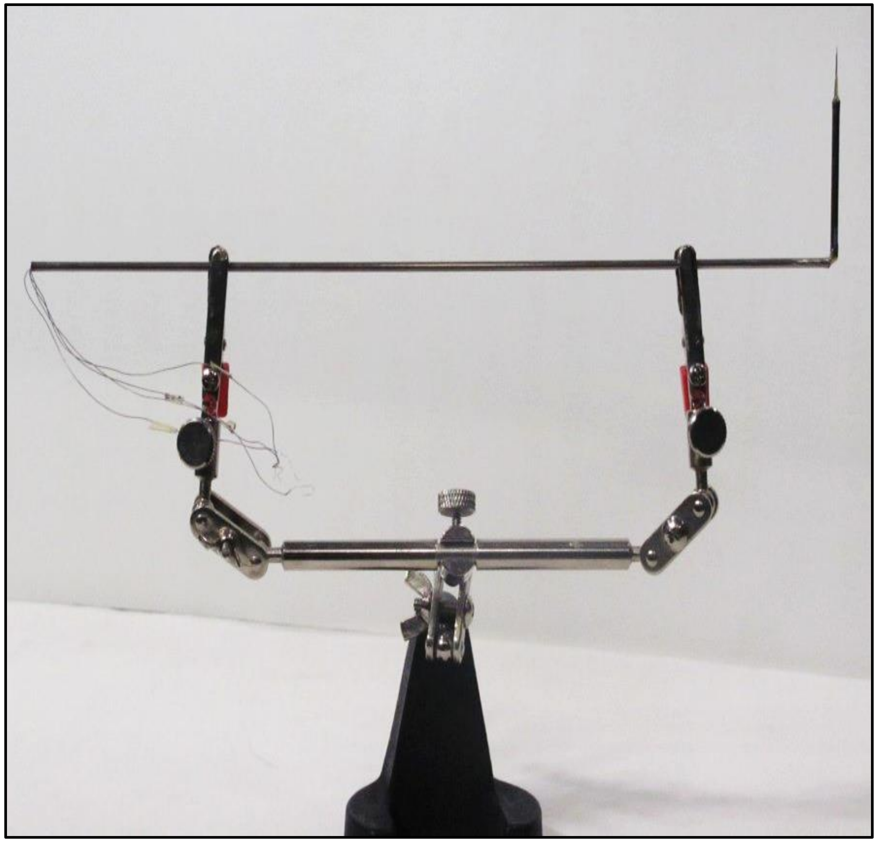

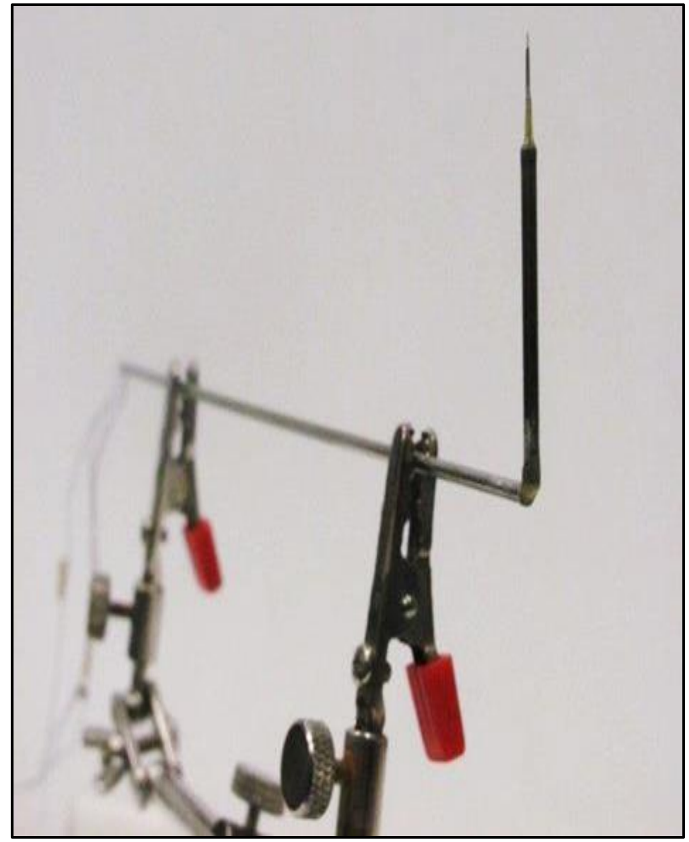

A four-sensor conductivity probe collects local data as it moves across the pipe with a specialized measurement port.

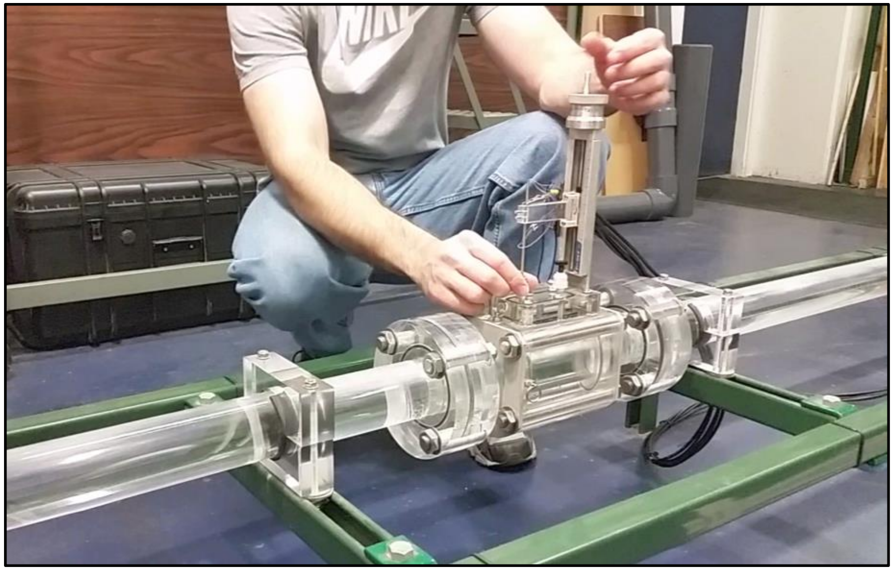

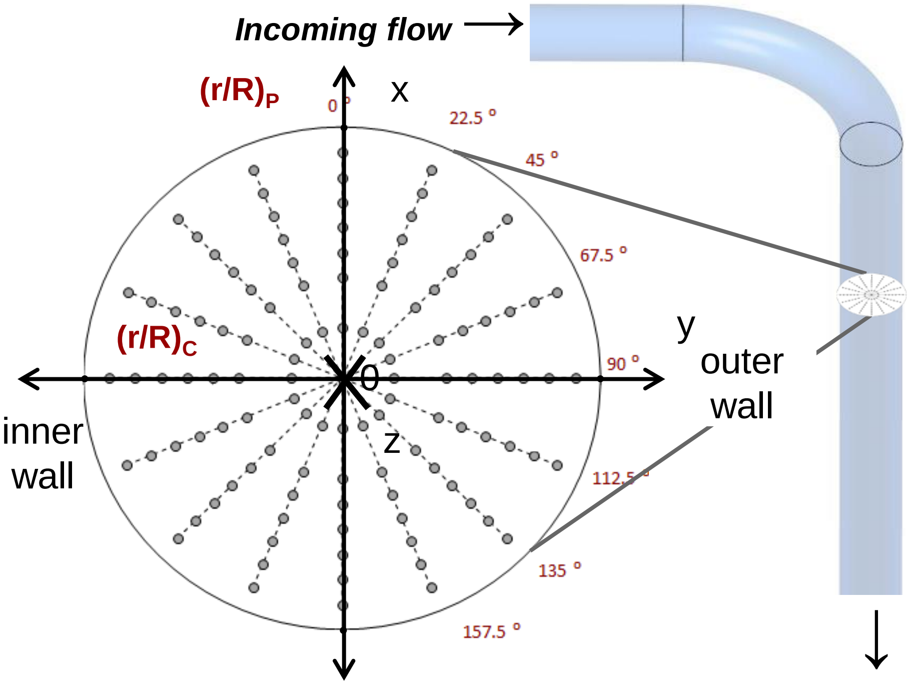

120 data points/cross-section

New experimental data was collected at 0D and 3D after the vertical-downward elbow.

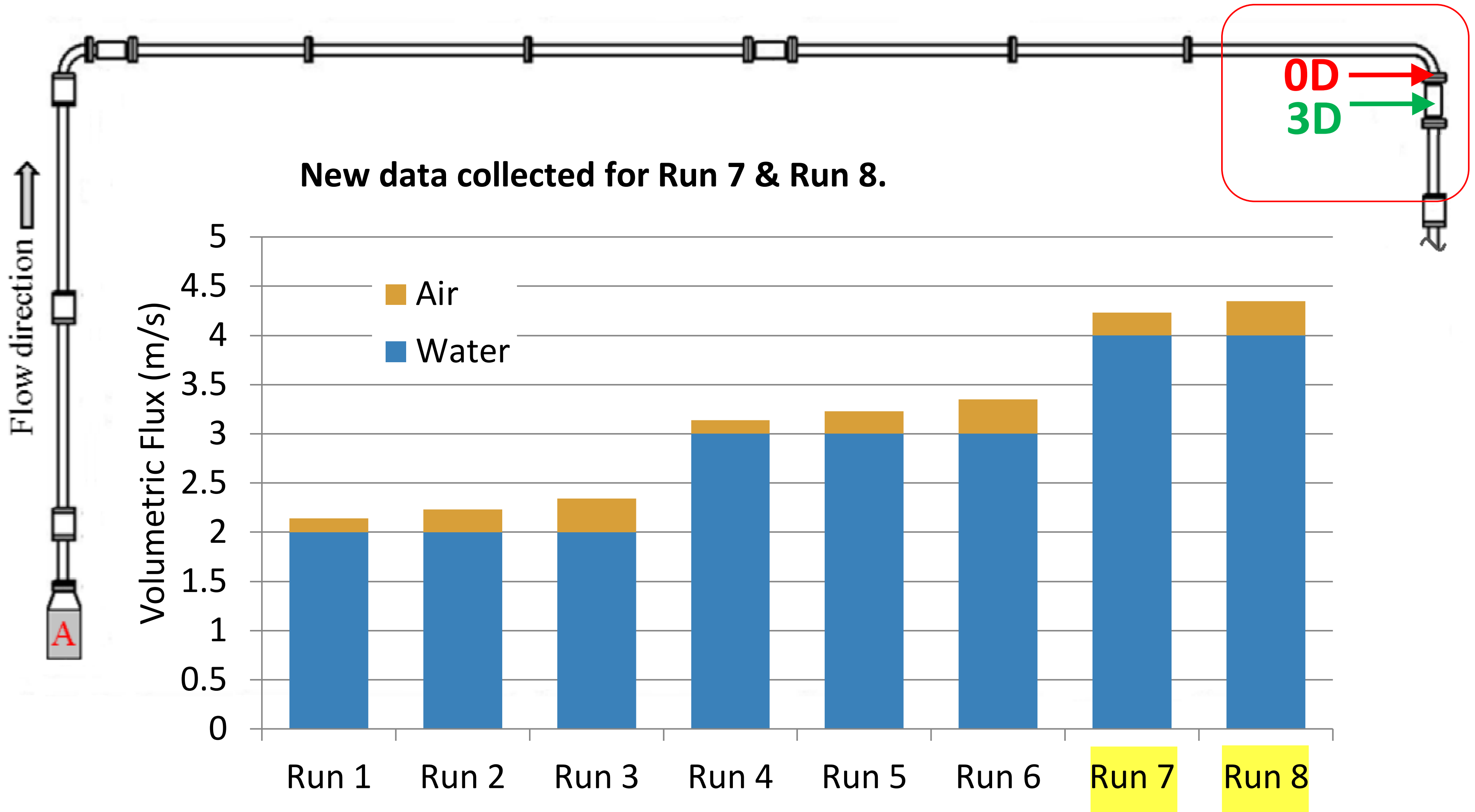

Void fraction is measured with the conductivity probe in order to better understand two-phase flow structure.

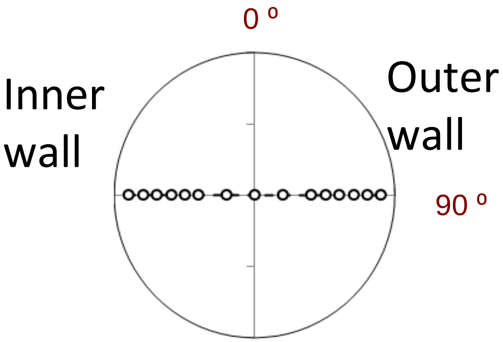

<u>Run 7</u>

J_f : 4.00 m/s

$J_{g,\,atm}$: 0.23 m/s

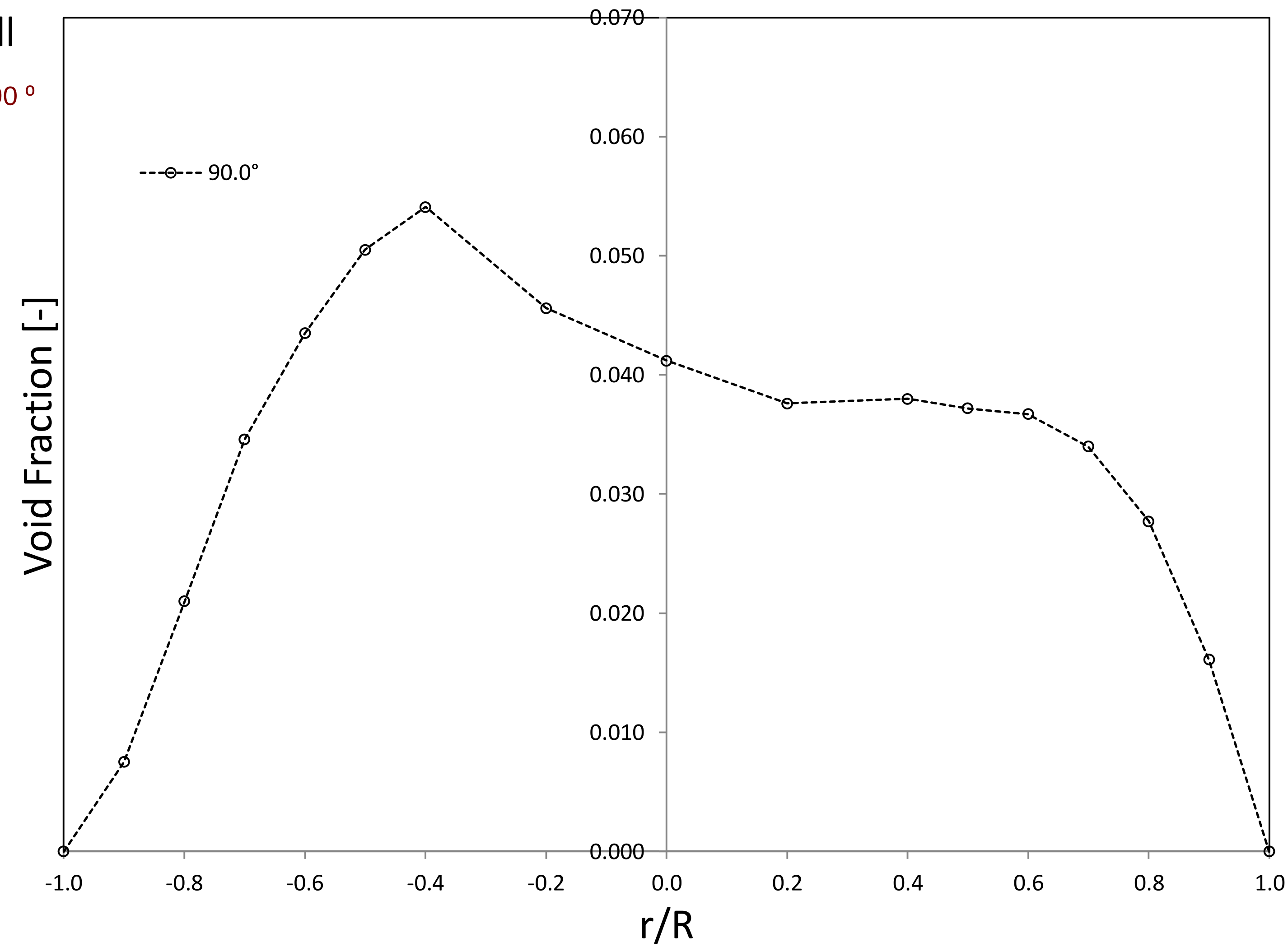

Void fraction is measured with the conductivity probe in order to better understand two-phase flow structure.

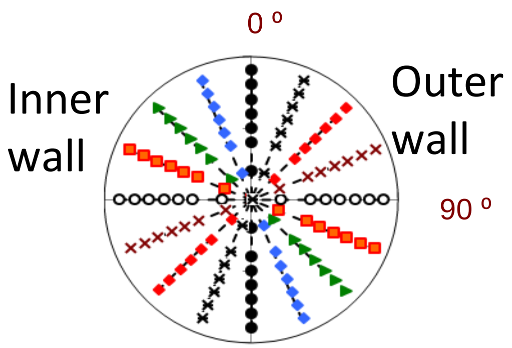

<u>Run 7</u>
J_f : 4.00 m/s
$J_{g,\,atm}$: 0.23 m/s

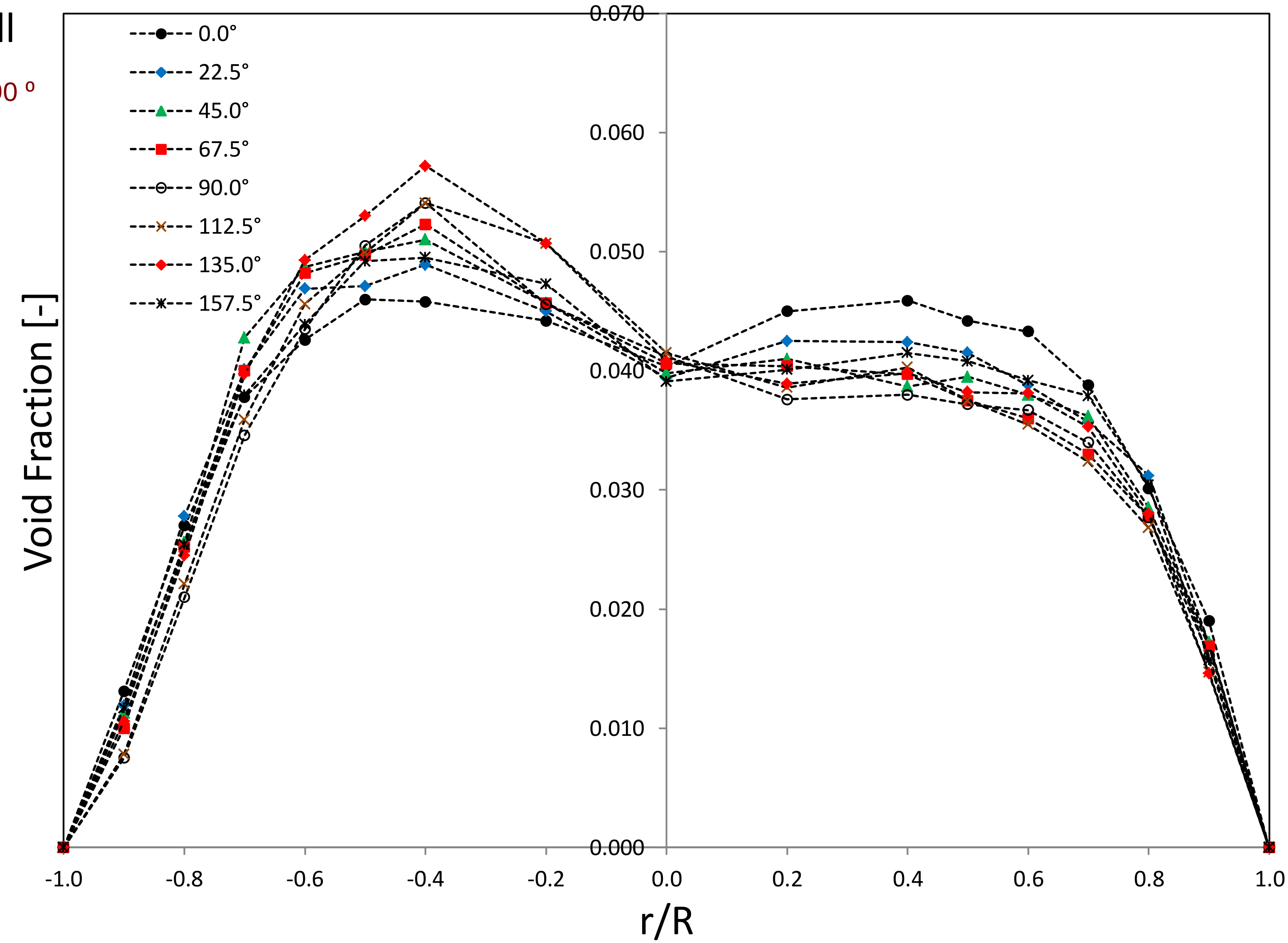

The void fraction distribution reveals a single peak after the vertical-downward elbow.

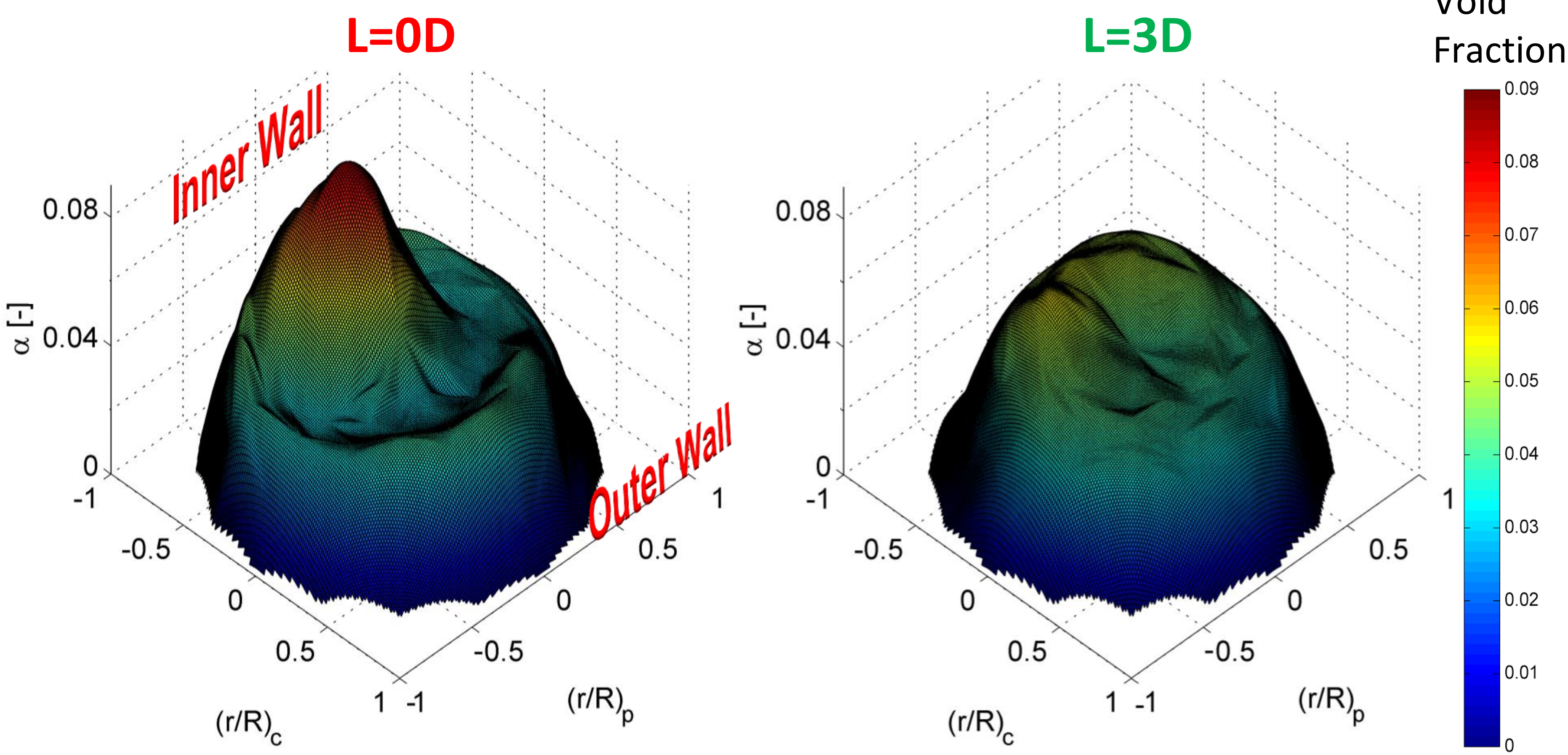

Run 7

Volumetric liquid flux: 4.00 m/s
Volumetric gas flux: 0.23 m/s

The void fraction distribution reveals a single peak after the vertical-downward elbow.

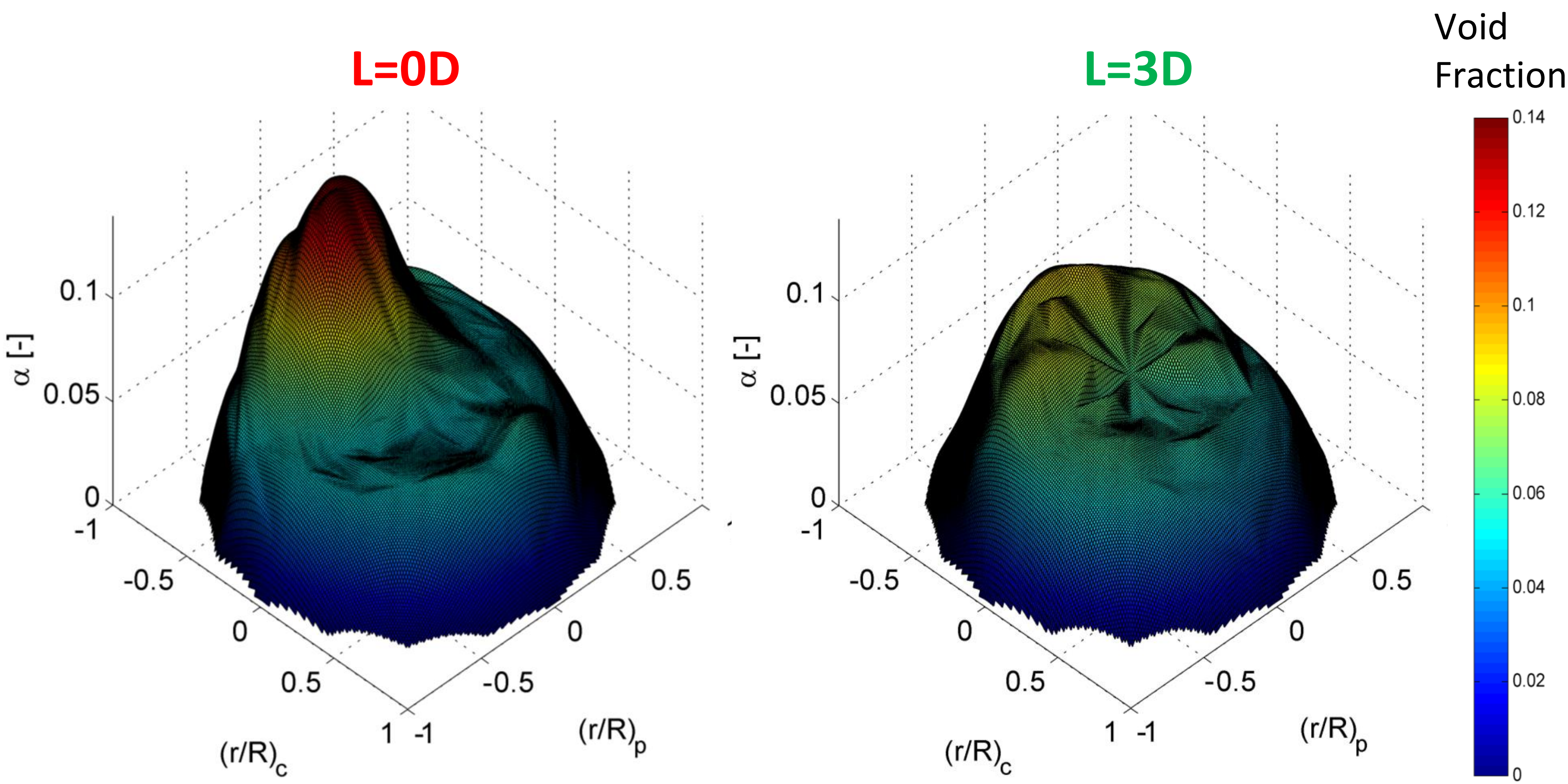

Run 8

Volumetric liquid flux: 4.00 m/s
Volumetric gas flux: 0.35 m/s

When compared, void fraction distribution and secondary flow show different flow characteristics.

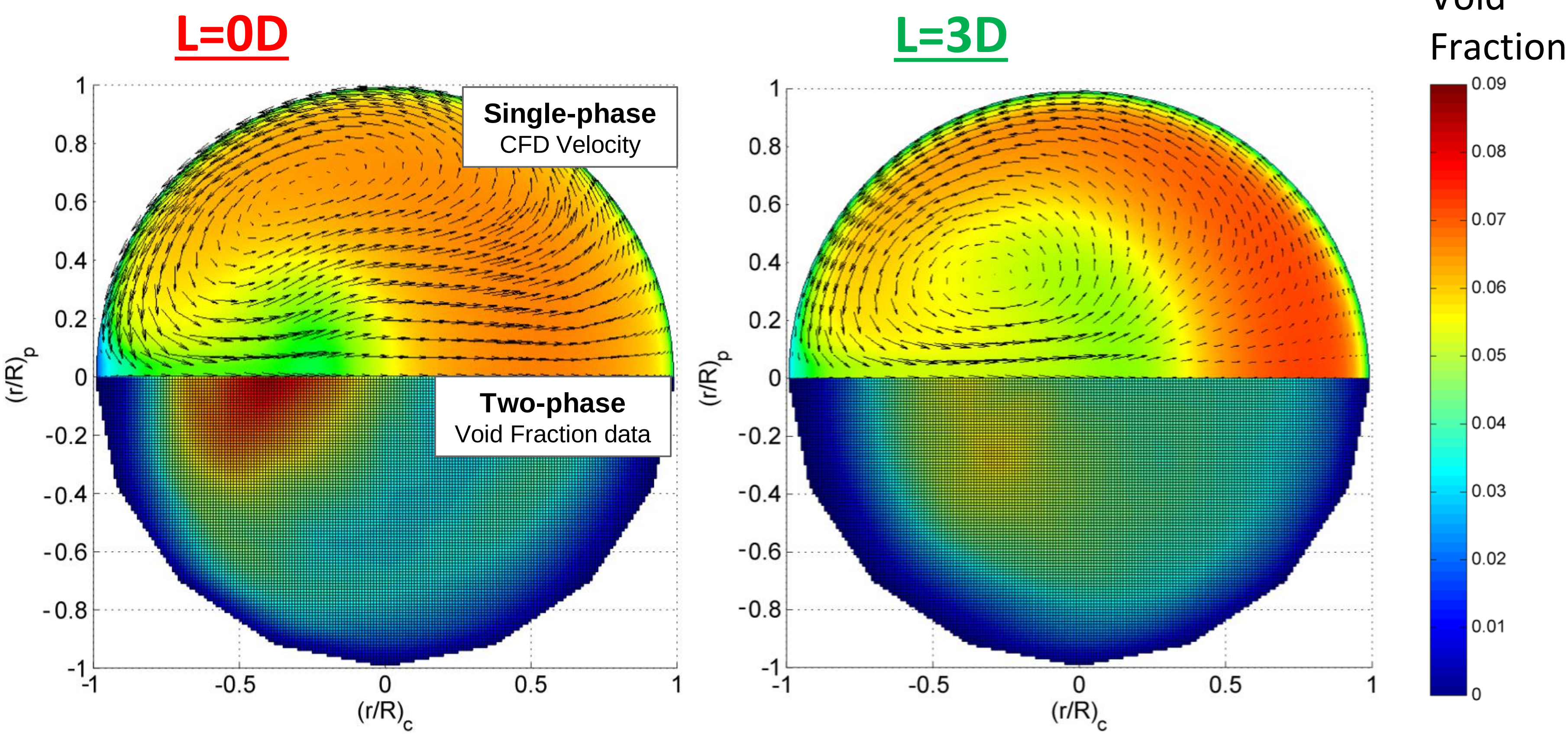

Run 7

Volumetric liquid flux: 4.00 m/s
Volumetric gas flux: 0.23 m/s

When compared, void fraction distribution and secondary flow show different flow characteristics.

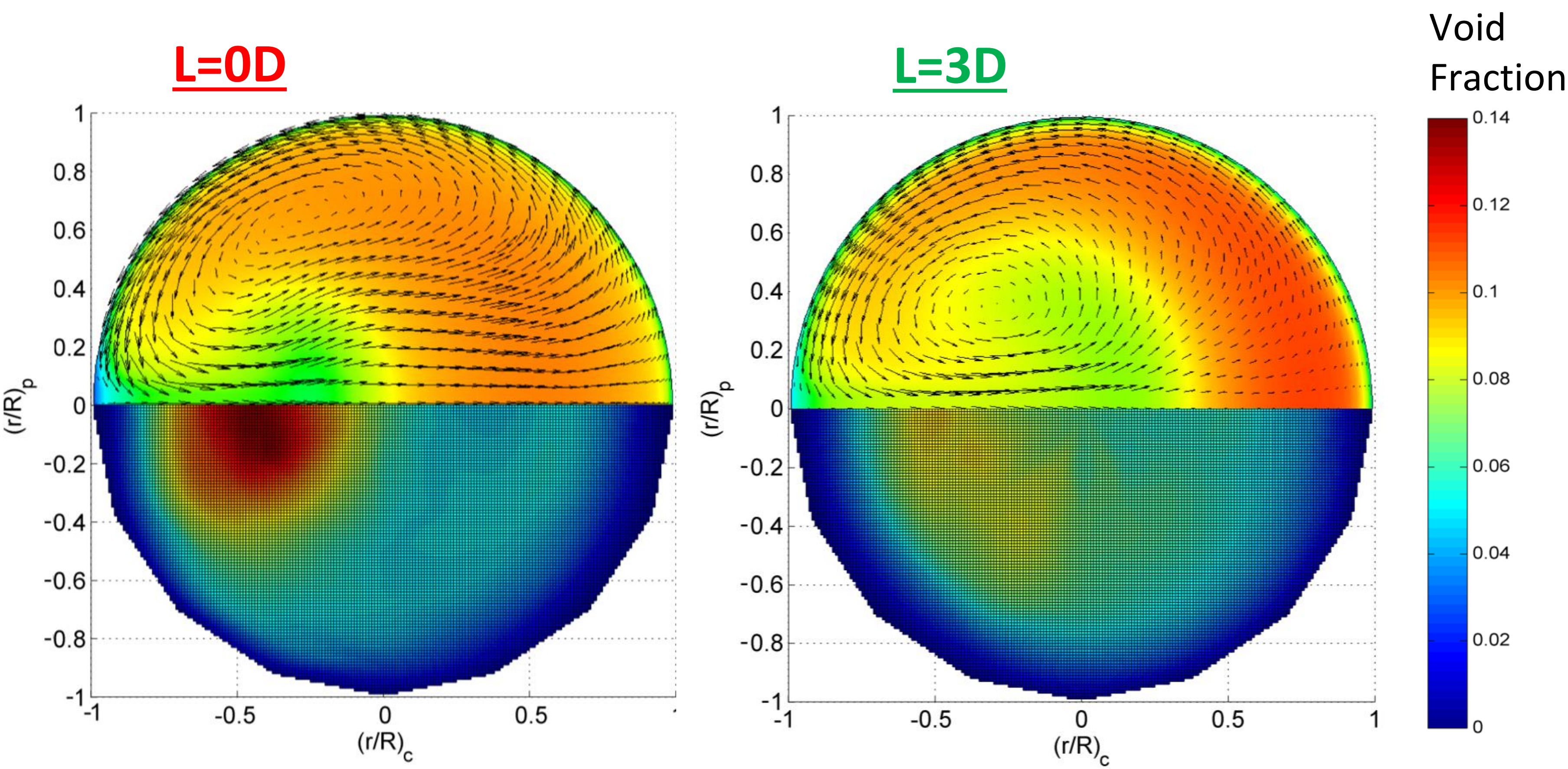

Run 8

Volumetric liquid flux: 4.00 m/s
Volumetric gas flux: 0.35 m/s

Swirling has a different impact after the vertical-downward elbow in comparison to the vertical-upward elbow.

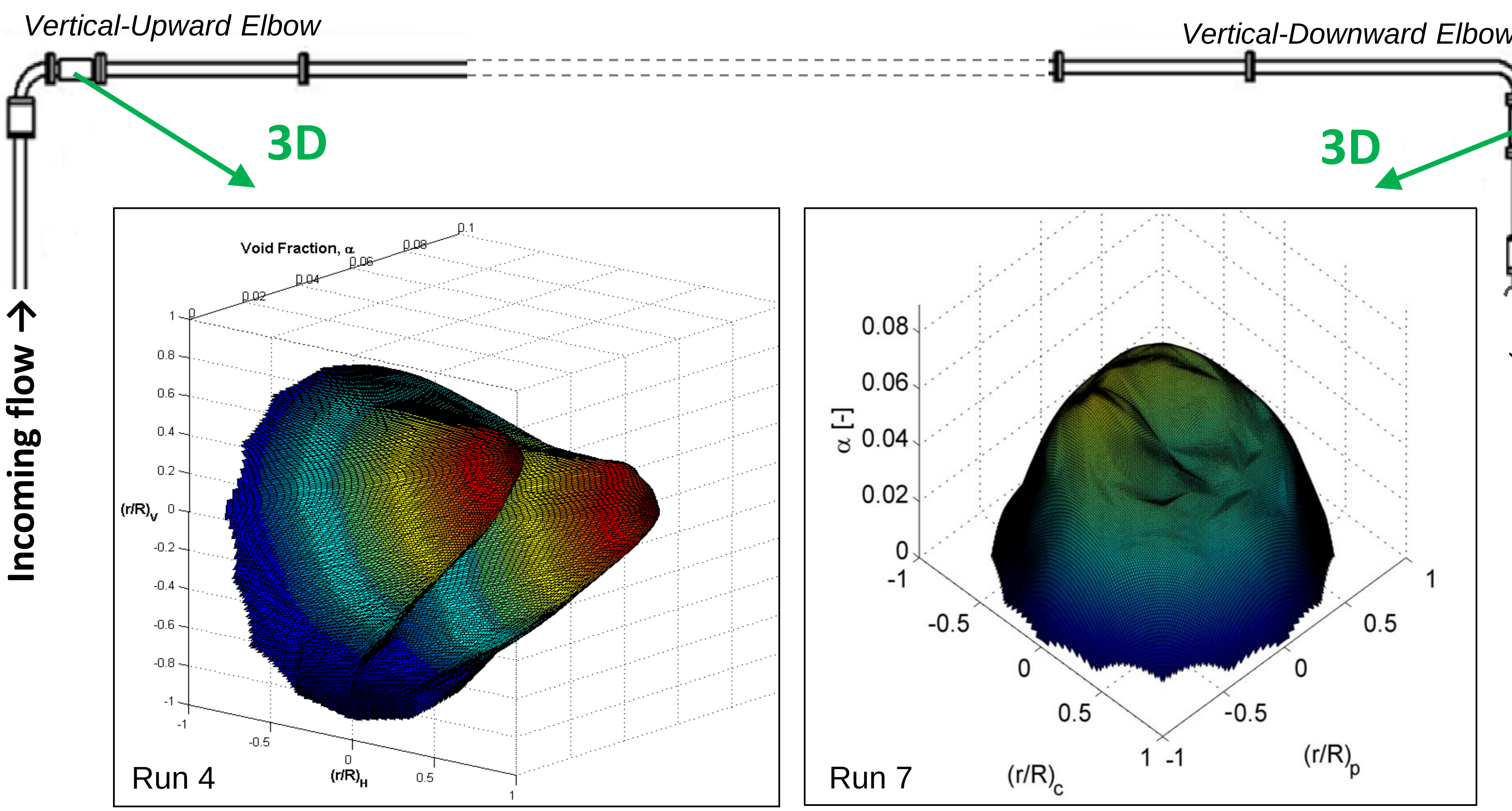

Swirling has a different impact after the vertical-downward elbow in comparison to the vertical-upward elbow.

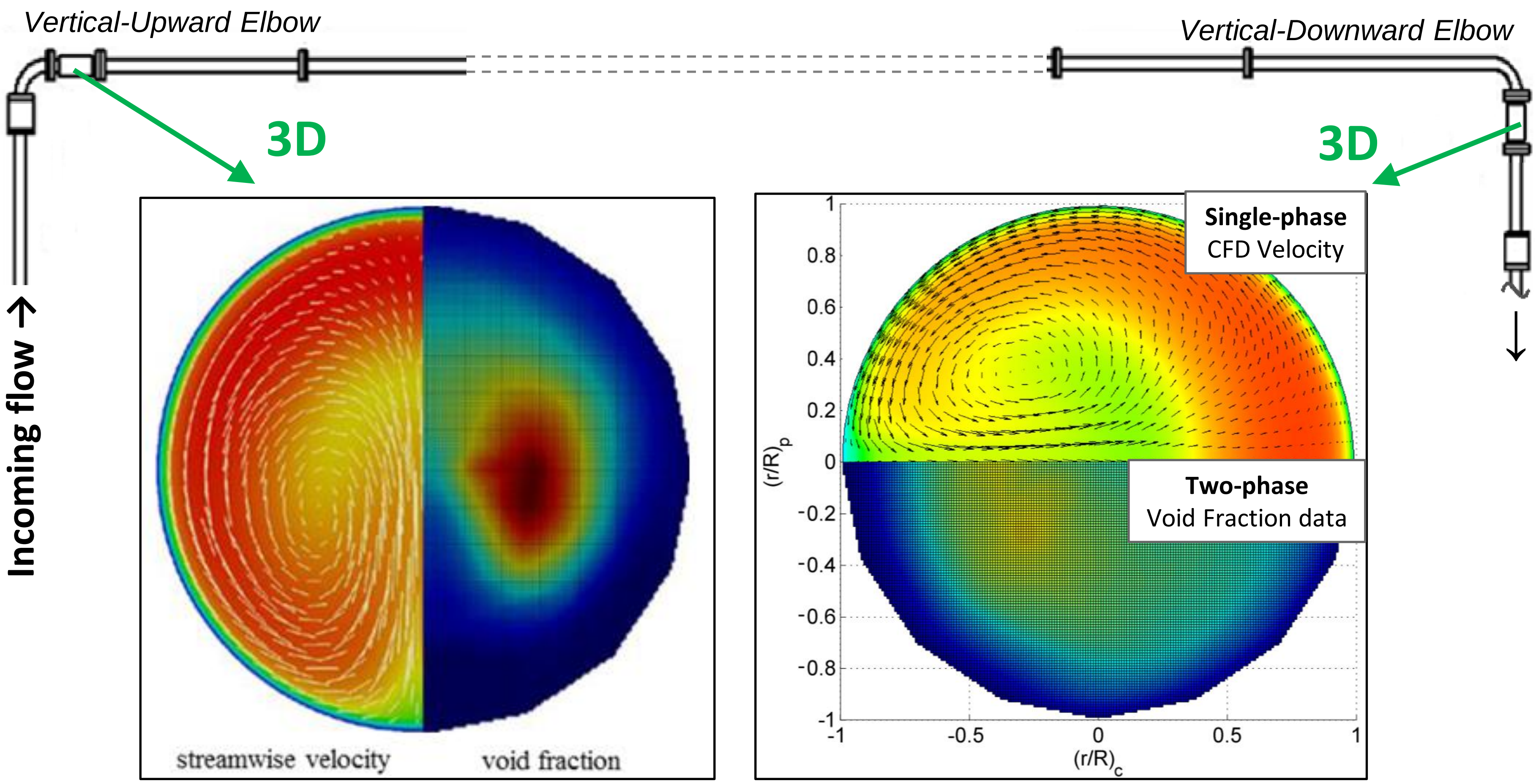

Our reasearch provides new data and results for the vertical-downward elbow for future reactor safety.

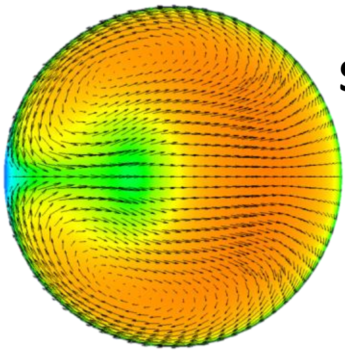

Single-phase CFD analysis

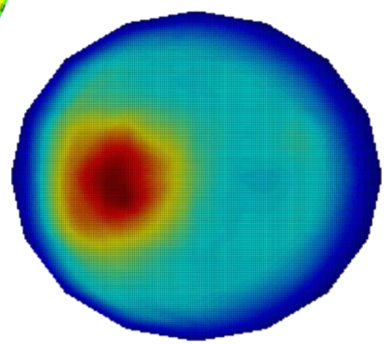

Establish Database

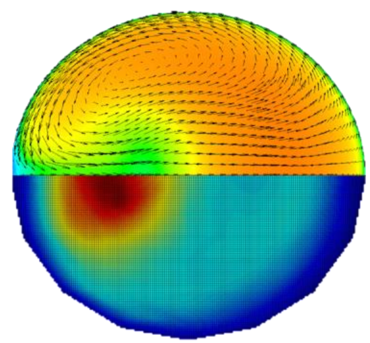

Comparison

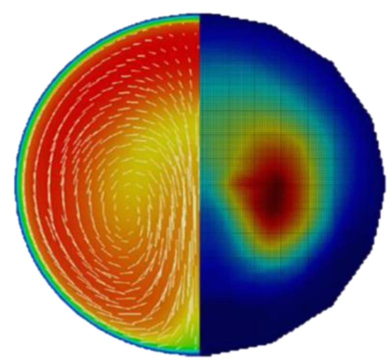

Previous Studies Comparison

Questions?

ADDITIONAL SLIDES

Acknowledgements

Special thanks to **Toshiba Westinghouse** for generously funding this Undergraduate Fellows Program.

Lori Miraldi
Lecturer in Communication Arts and Sciences
Department of Communications Arts and Sciences
The Pennsylvania State University
lorimiraldi@psu.edu

Dr. Seungjin Kim
Associate Professor of Mechanical and Nuclear Engineering
Department of Mechanical and Nuclear Engineering
The Pennsylvania State University
skim@psu.edu

Shouxu Qiao
Ph. D. Student
The Pennsylvania State University
szq105@psu.edu

Questions?

Recommendations for future work

- Obtain more data for database of different flow rates and locations.
- Develop predictive models for two-phase flow around restrictions.
- Implement new models to reactor system analysis code for higher safety.

References

A. Das, S.M. Ishtiaque, S.N. Singh, and A. Gupta, “Optimization of fluid flow inside blowroom transport duct using CFD,” Journal of the Textile Institute, pp. 1–12, 2014.

Kim, S., Fu, X. Y., Wang, X., & Ishii, M. (2000). Development of the miniaturized four-sensor conductivity probe and the signal processing scheme. International Journal of Heat and Mass Transfer, 43(22), 4101-4118. doi:10.1016/S0017-9310(00)00046-6

Crawford, N. M., Cunningham, G., & Spence, S. W. T. (2007). An experimental investigation into the pressure drop for turbulent flow in 90° elbow bends. Proceedings of the Institution of Mechanical Engineers, Part E: Journal of Process Mechanical Engineering, 221(2), 77-88. doi:10.1243/0954408JPME84

Ishii, M., Hibiki, T., & SpringerLink (Online service). (2006). Thermo-fluid dynamics of two-phase flow. New York, N.Y: Springer Science+Business Media.

Yadav, M. S., & Kim, S. (2013). Interfacial area transport across vertical elbows in air-water two-phase flow. Pennsylvania State University. University Park, Pa.

Yadav, M., & Kim, S. (2013). EFFECTS OF 90-deg VERTICAL ELBOWS ON THE DISTRIBUTION OF LOCAL TWO-PHASE FLOW PARAMETERS. Nuclear Technology, 181(1), 94-105.

Yadav, M., Worosz, T., Kim, S., Tien, K., & Bajorek, S. (2014). Characterization of the dissipation of elbow effects in bubbly two-phase flows. International Journal of Multiphase Flow, 66, 101-109. doi:10.1016/j.ijmultiphaseflow.2014.07.0

Kim, J., Yadav, M., & Kim, S. (2014). Characteristics of secondary flow induced by 90-degree elbow in turbulent pipe flow. Engineering Applications of Computational Fluid Mechanics, 8(2), 229-239. doi:10.1080/19942060.2014.11015509

This slide shows the measurement principle of the four-sensor conductivity probe.

- Measurement principle: conductivity difference between gas and liquid phases

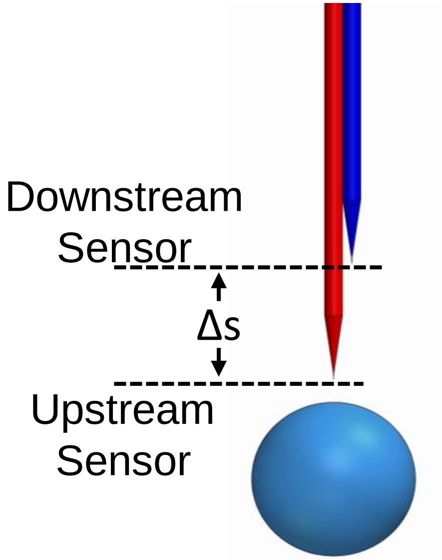

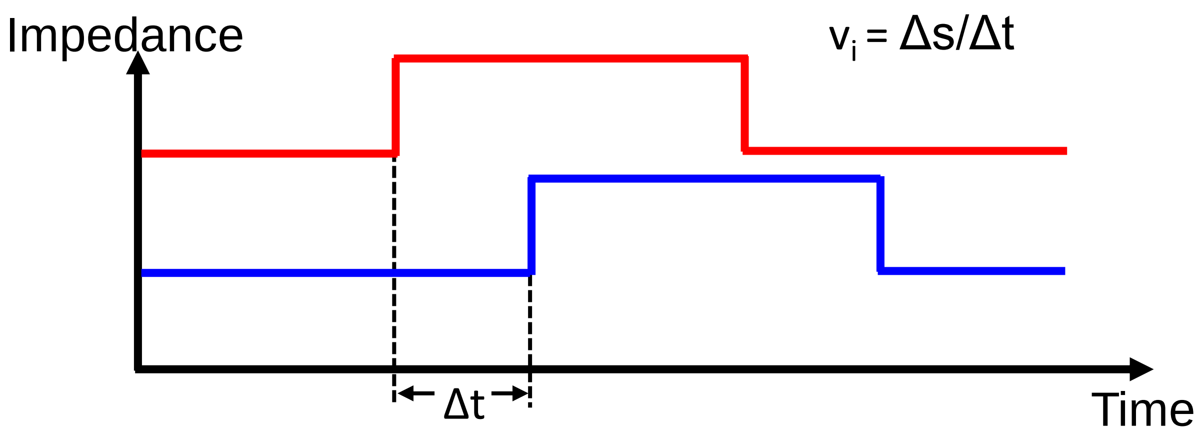

Local Time-Averaged a_i (Ishii, 1975): $$\overline{a}_i^t = \frac{1}{\Delta T}\sum_j \left(\frac{1}{|\vec{v}_i \cdot \vec{n}_i|}\right)_j$$

The state-of-the-art four-sensory conductivity probe creates minimal distortion of bubbles.

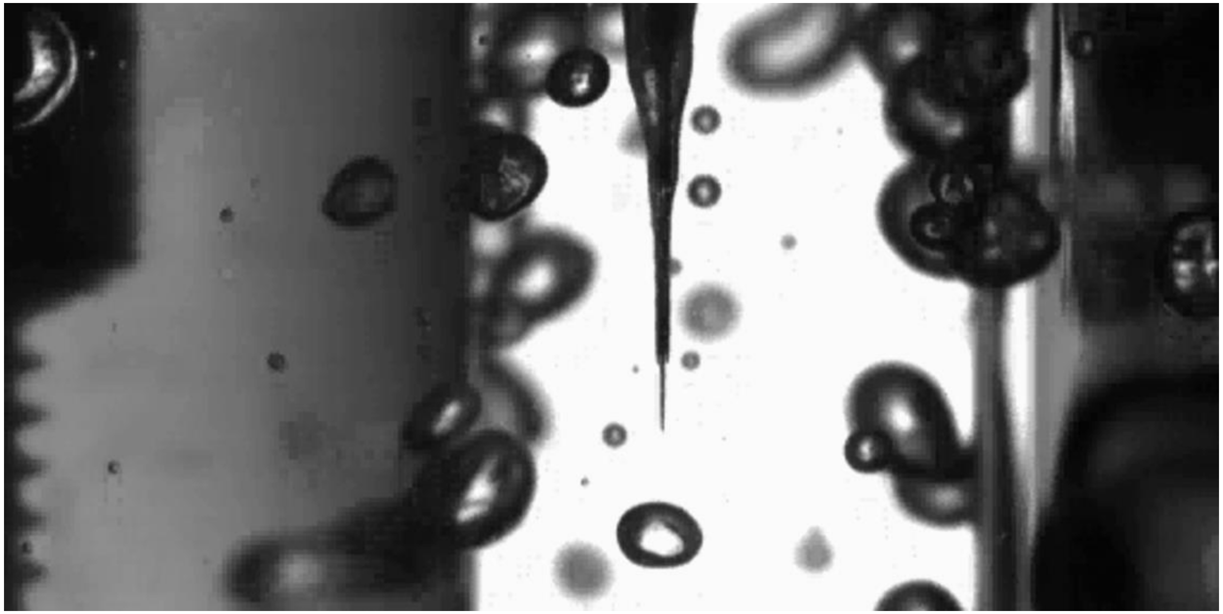

4000 fps

These images show the size and configuration of the four-sensor conductivity probe.

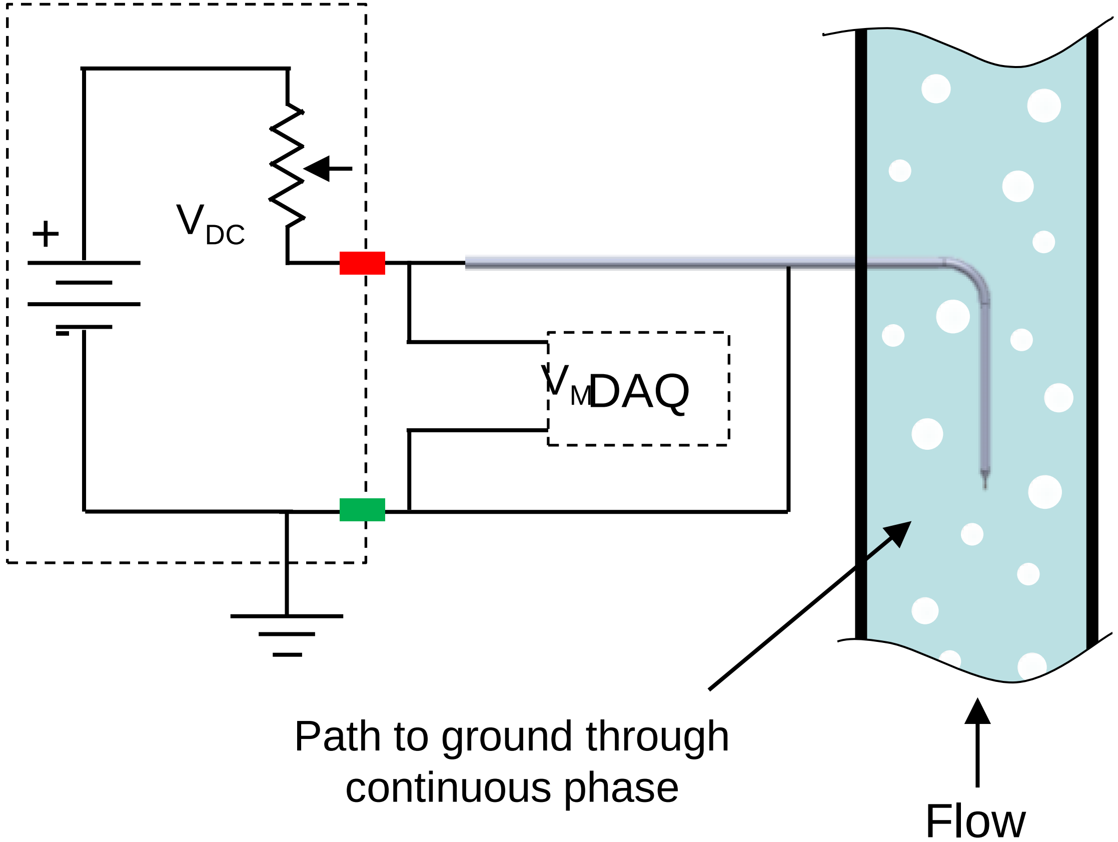

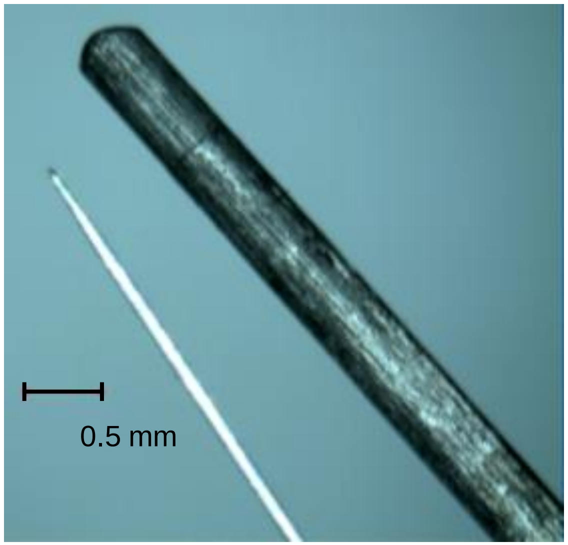

Acupuncture needle and 0.5 mm pencil lead

A mesh was generated for the loop geometry; this mesh was used as an input to the CFD solver.

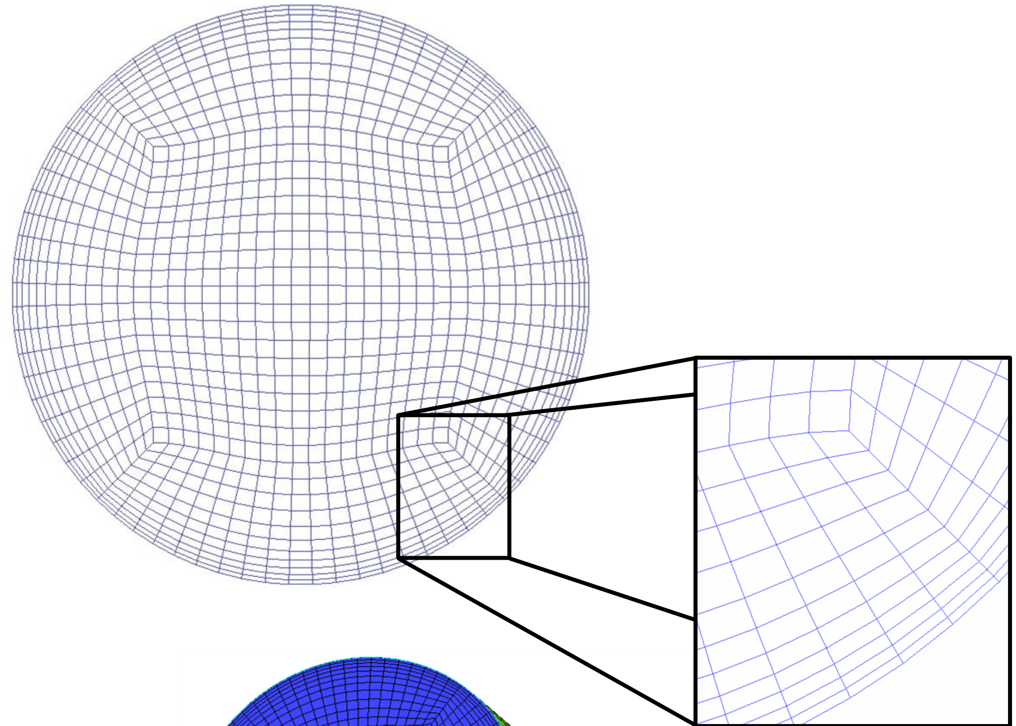

Accurate solutions require a well-constructed mesh.

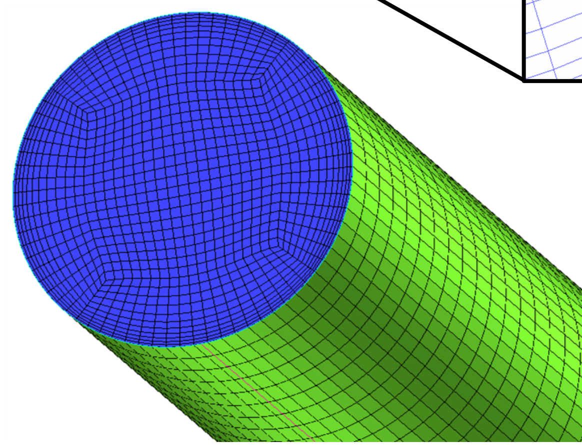

A mesh-sensitivity test confirmed that our results are grid-independent.

We have created high quality mesh to ensure accurate modeling

Geometry accurately represents the test facility

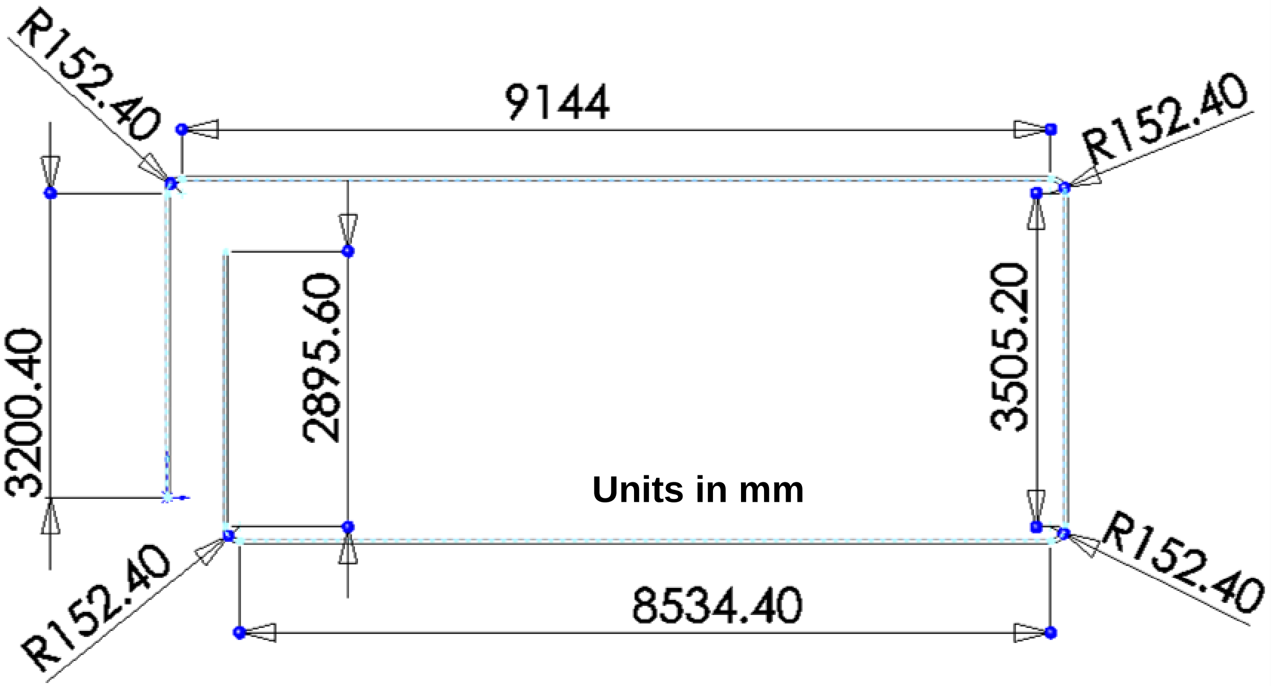

Structured O-mesh

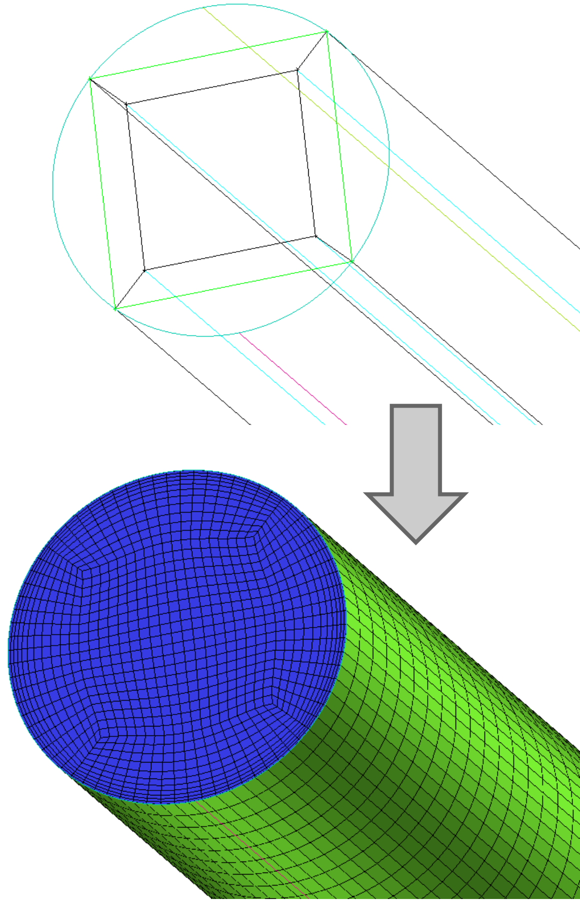

A mesh-sensitivity test demonstrates that our solution is grid-independent.

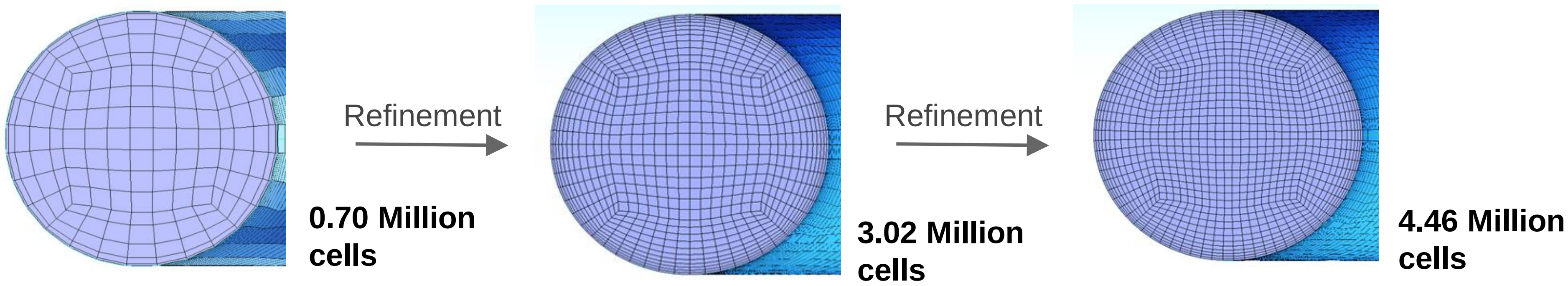

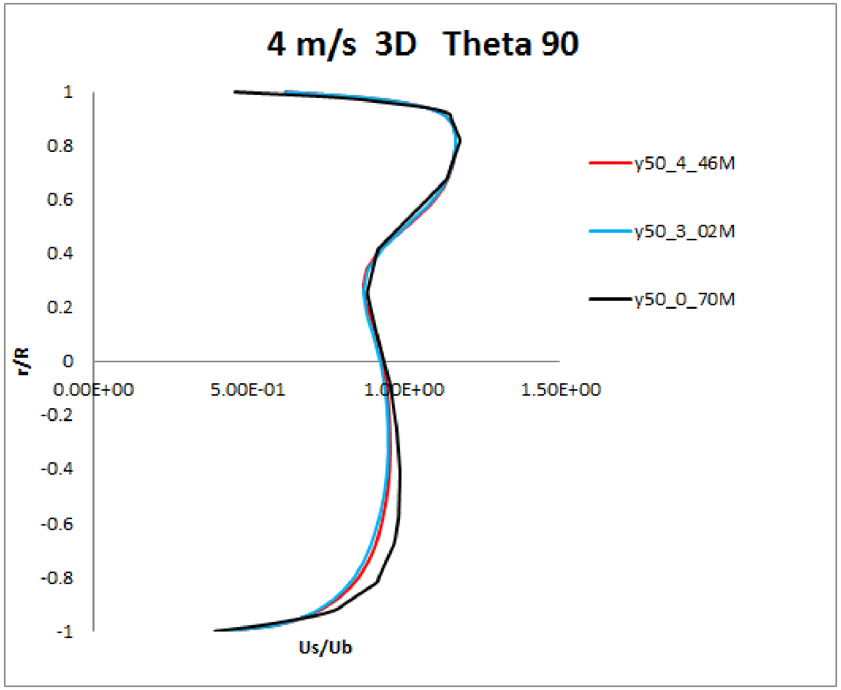

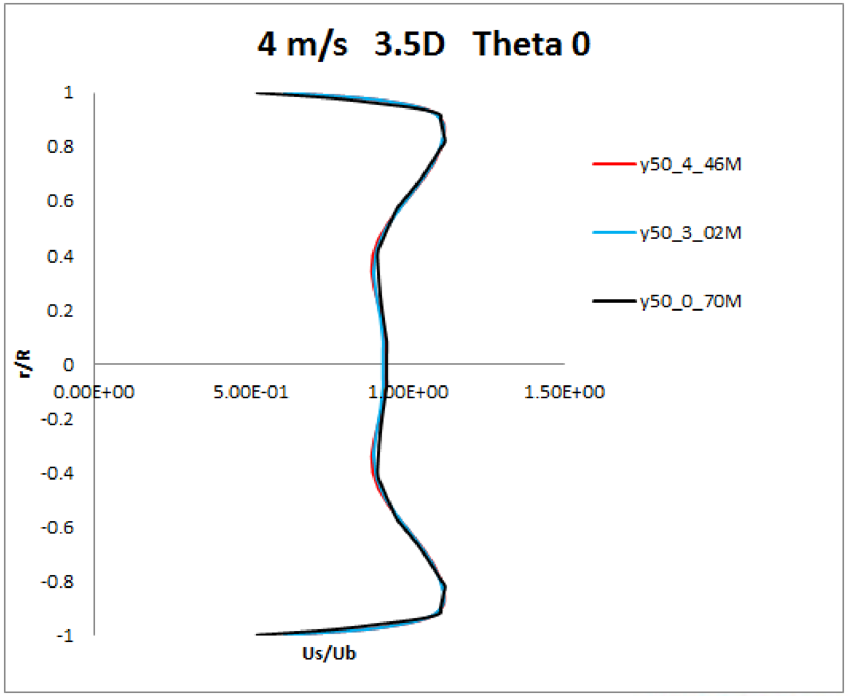

TOSHIBA
Westinghouse

The solution methods for our research compare well with previous research.

Kim, J., Yadav, M., & Kim, S. (2014). Characteristics of secondary flow induced by 90-degree elbow in turbulent pipe flow.

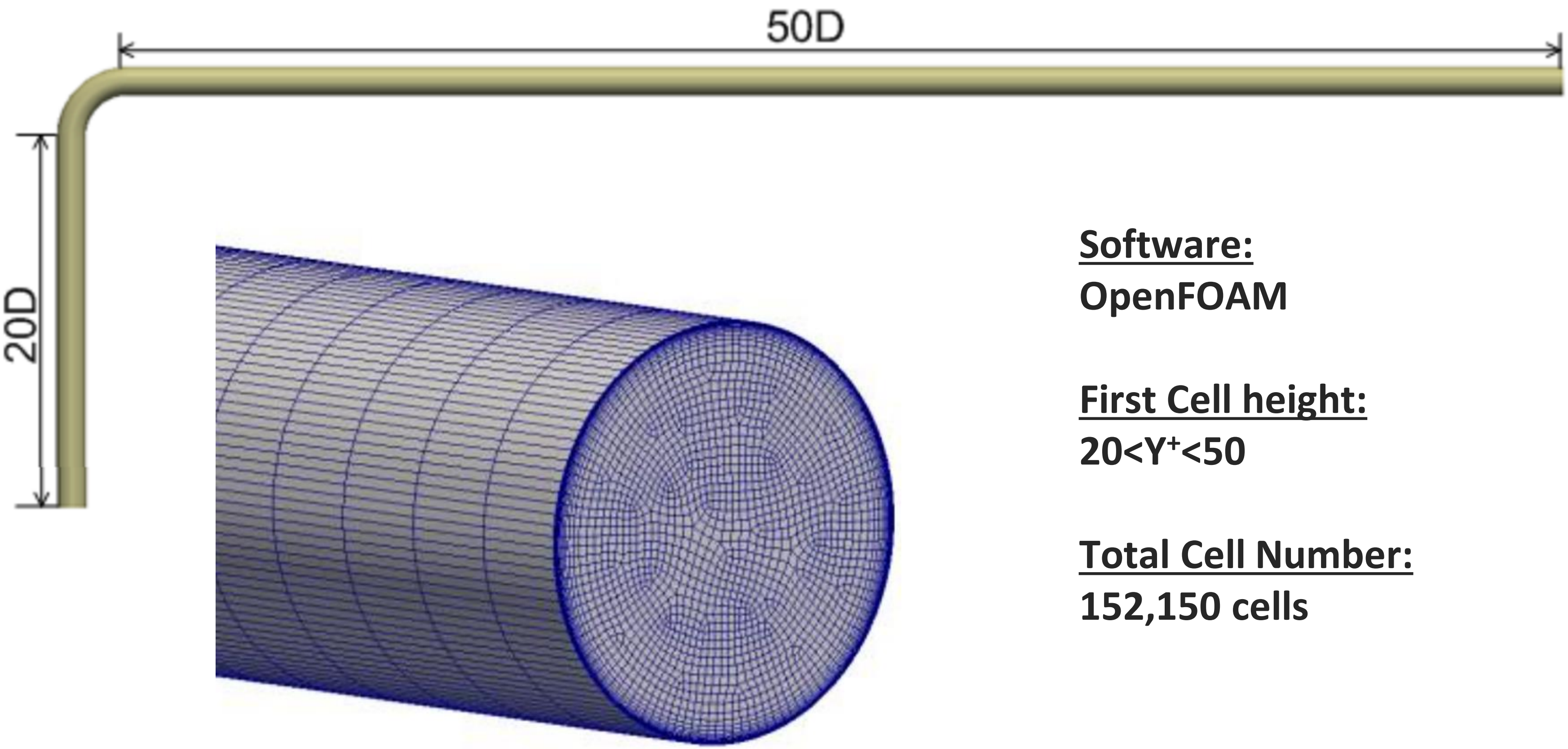

Fig. 3 Computational mesh near pipe exit.

Software:
OpenFOAM

First Cell height:
20<Y^+<50

Total Cell Number:
152,150 cells

Our results for the vertical-upward elbow were compared with previous research to confirm the accuracy of our simulations.

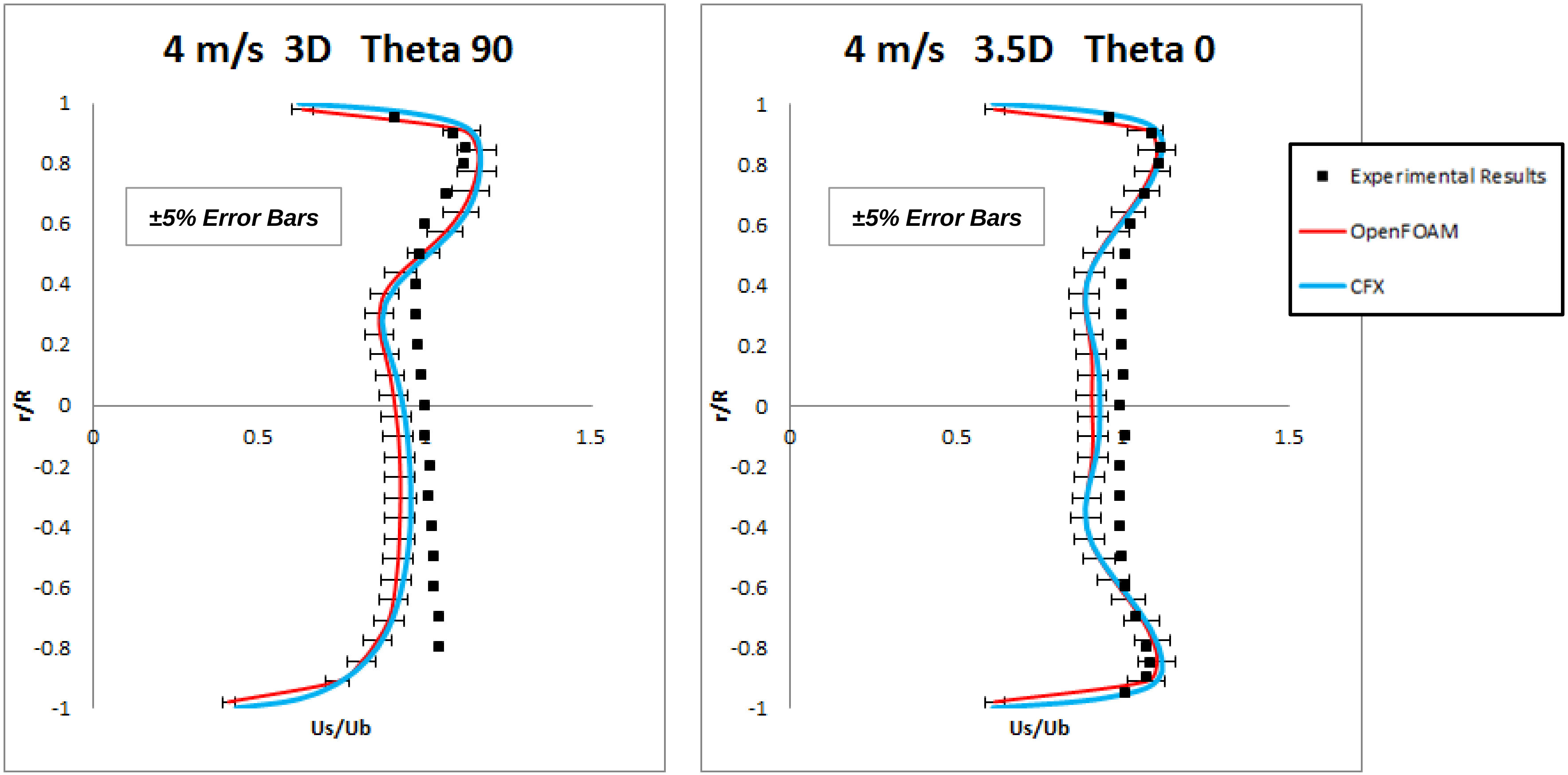

Secondary flow induced by elbow is seen to dissipate across nondimensional length through Swirl Intensity.

Swirl Intensity (I_s) is defined as:

$$I_s = \frac{\int \left[\vec{U} - (\vec{U} \cdot \hat{n})\hat{n}\right]^2 dA}{U_b^2 \int dA}$$

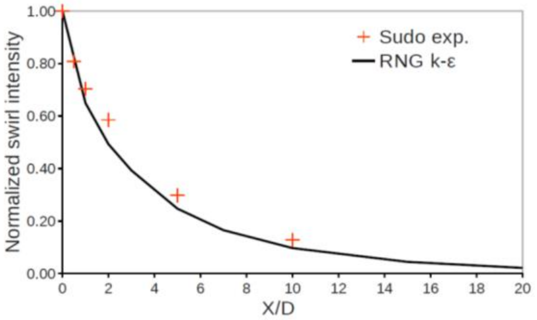

Fig. 17 Decay of swirl intensity along straight pipe after elbow with Rc = 2D.

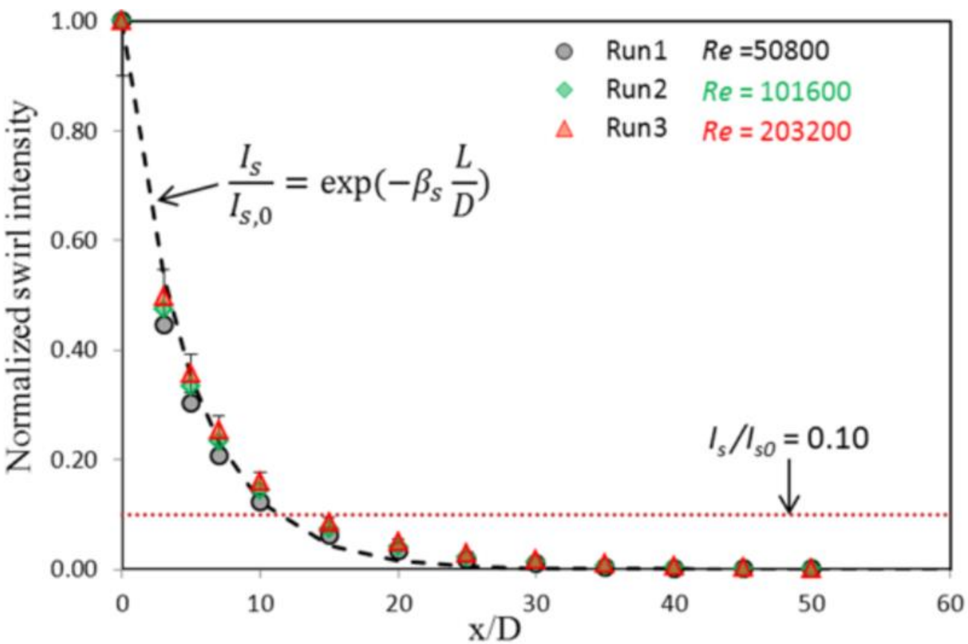

Fig. 18 Decay of normalized swirl intensity along pipe after elbow with Rc = 3D.

Kim et al. (2014) correlation:

$$\frac{I_s}{I_{s0}} = \exp(-\beta_s \frac{L}{D})$$

where β=0.21

Swirl Intensity measures the magnitude of secondary flow, which dissipates after an elbow.

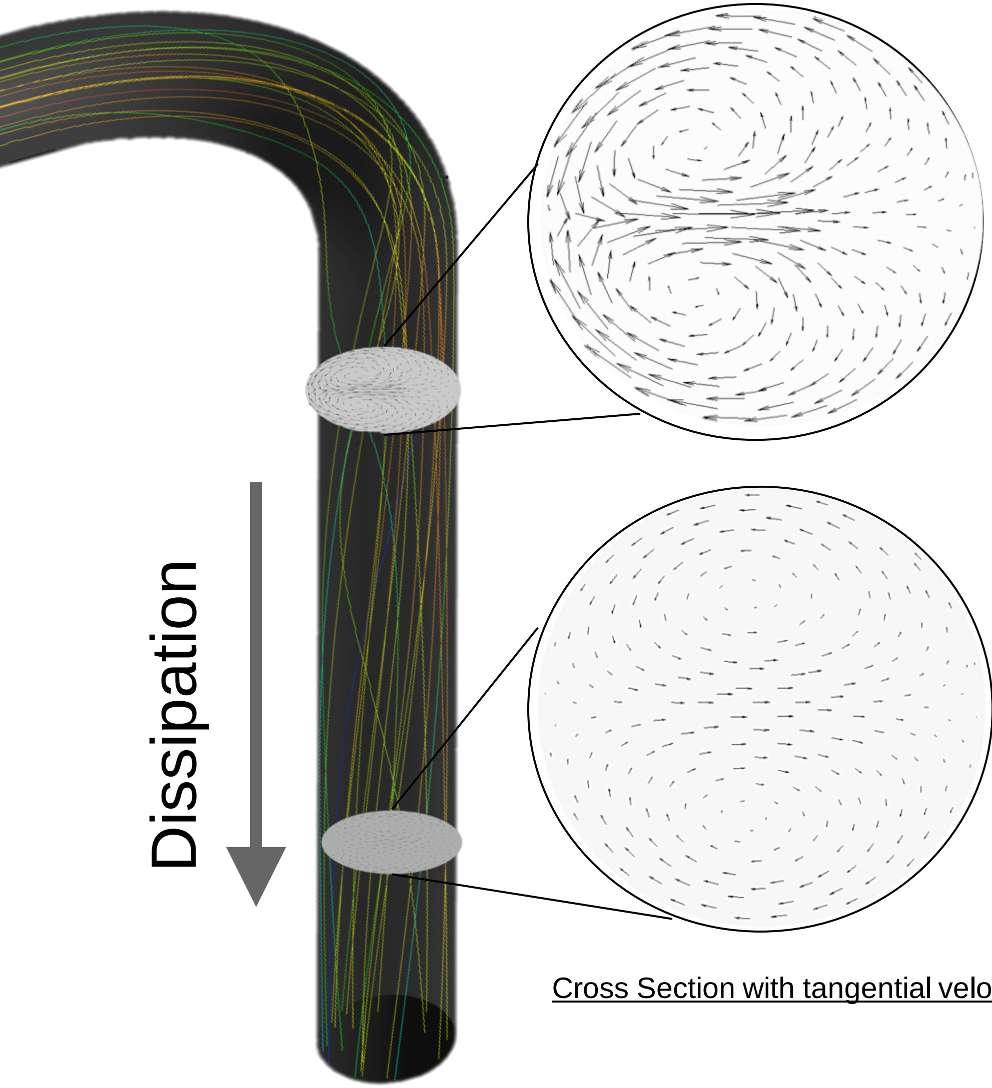

Cross Section with tangential velocity vectors

$$\textbf{Swirl Intensity} = \frac{\text{Average Tangential Velocity}}{\text{Average Axial Velocity}}$$

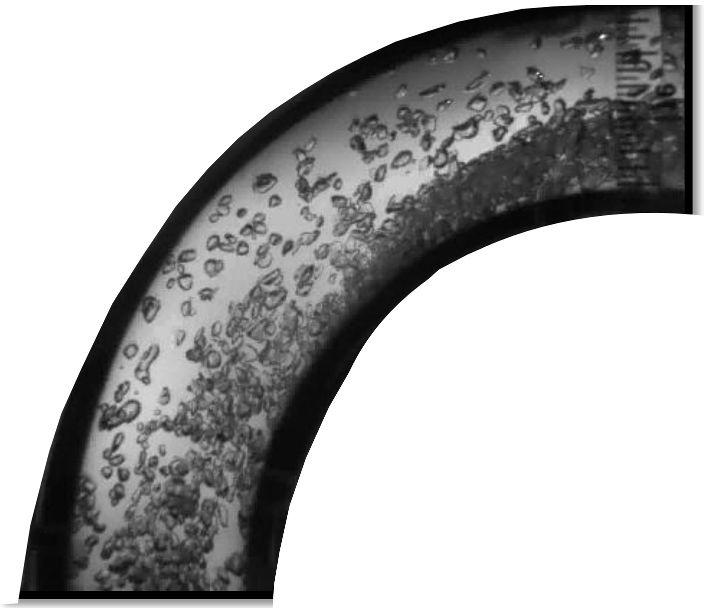

Swirl Intensity dissipates 90% by 15D after an elbow in CFX simulations.

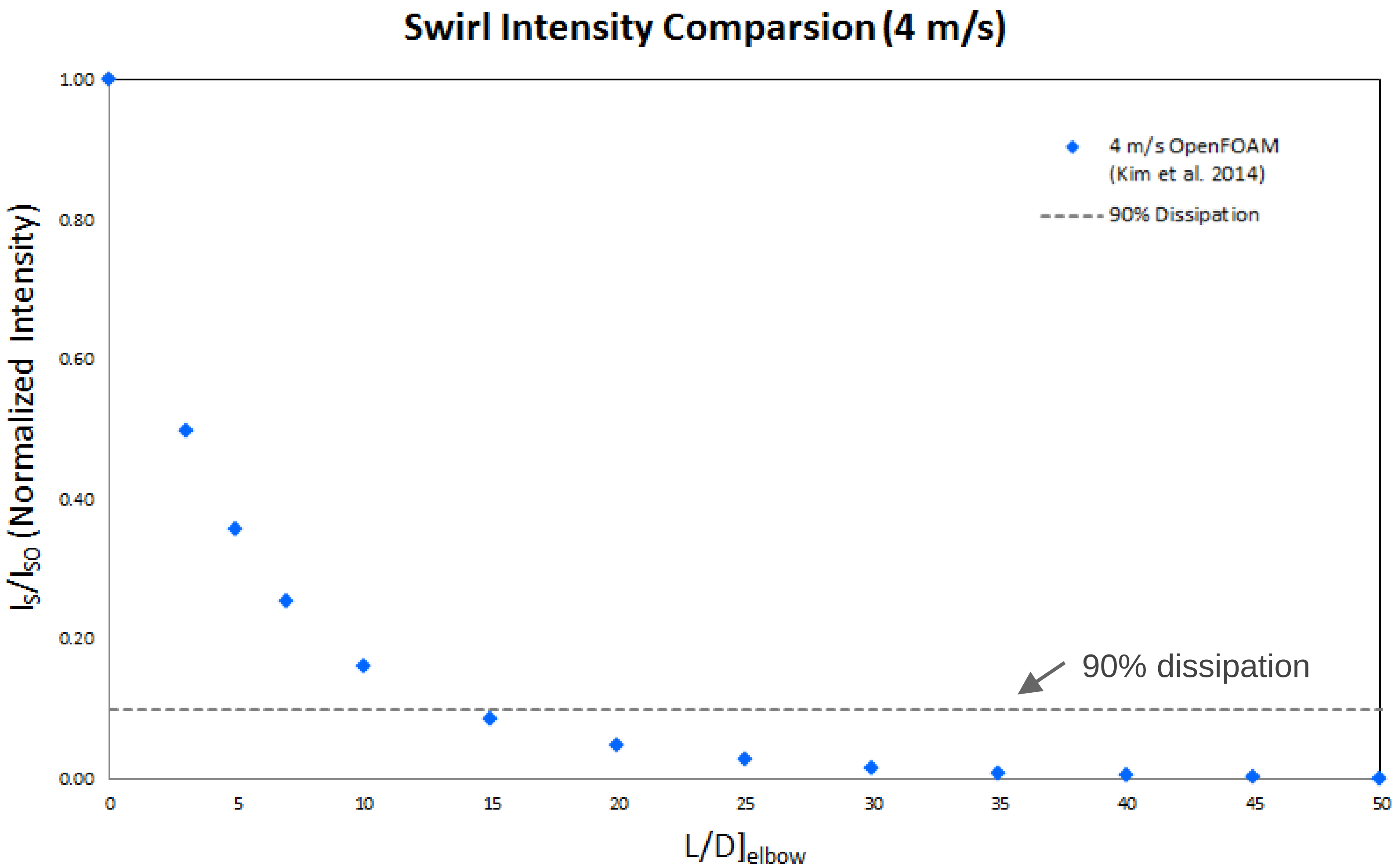

Swirl Intensity dissipates 90% by 15D after an elbow in CFX simulations.

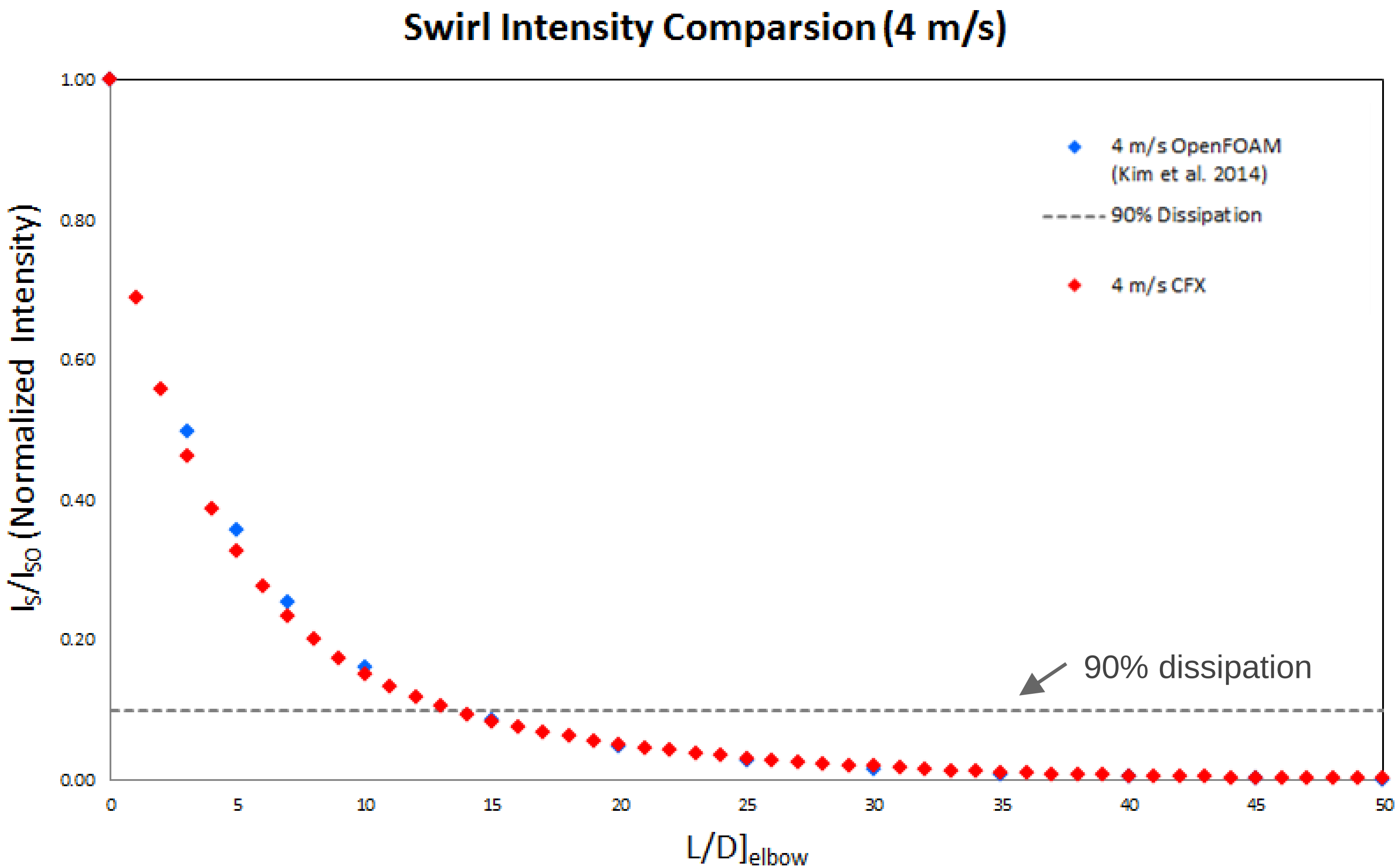

Swirl Intensity dissipation is independent of elbow orientation.

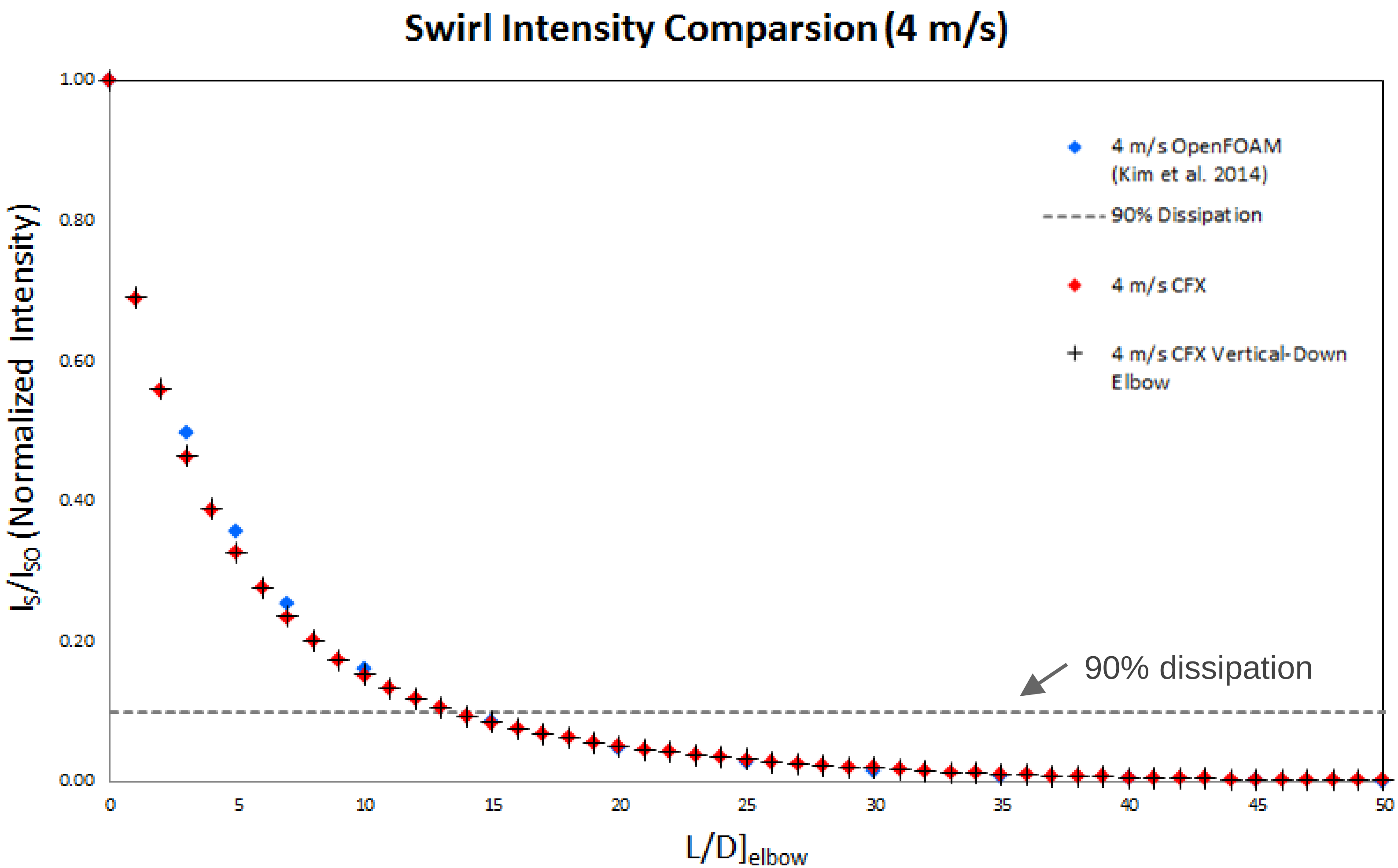

The CFX simulations match the Swirl Intensity decay of OpenFOAM results.

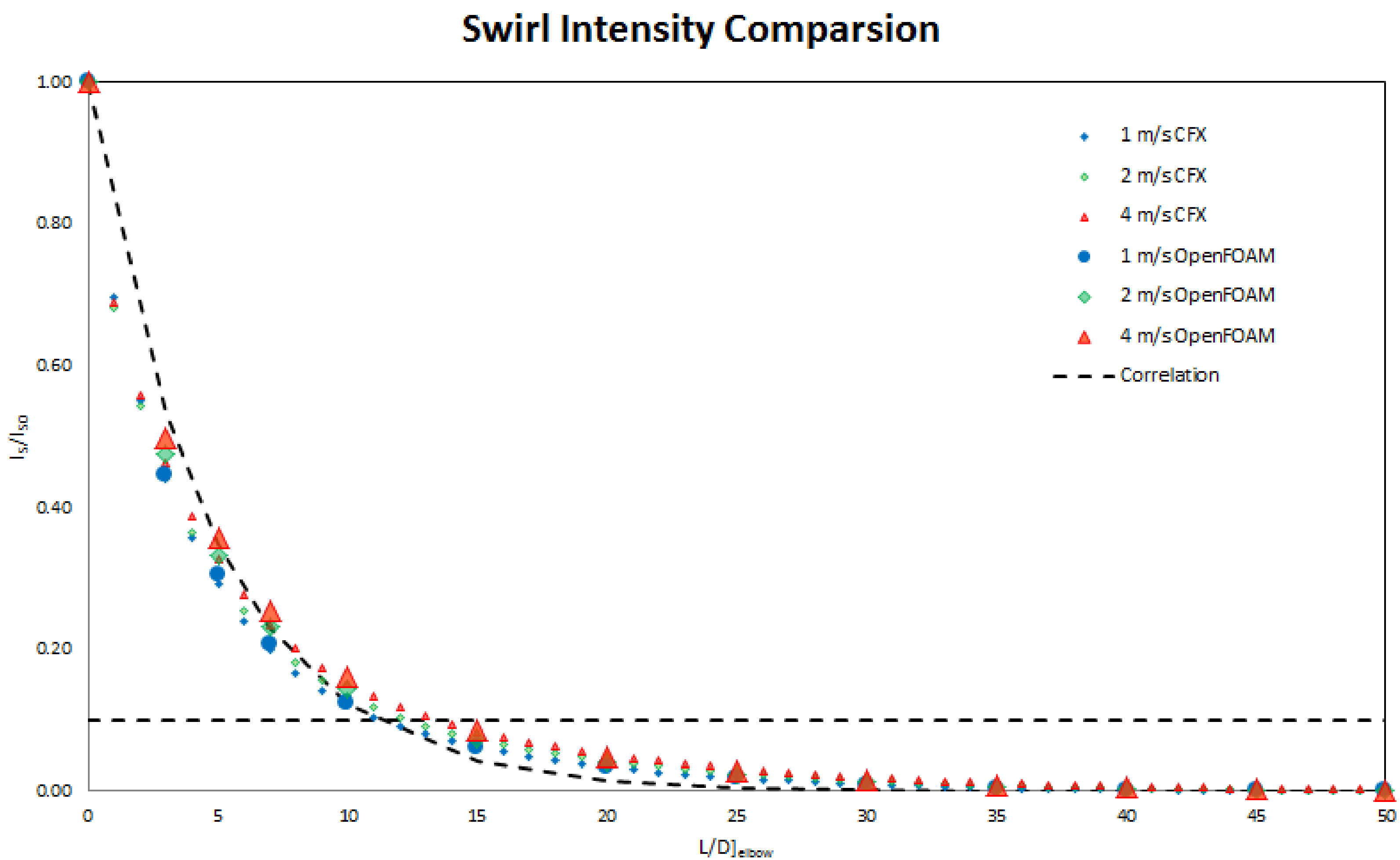

CFD models were analyzed at 0D, 3D, 10D, and 50D after the vertical-downward elbow.

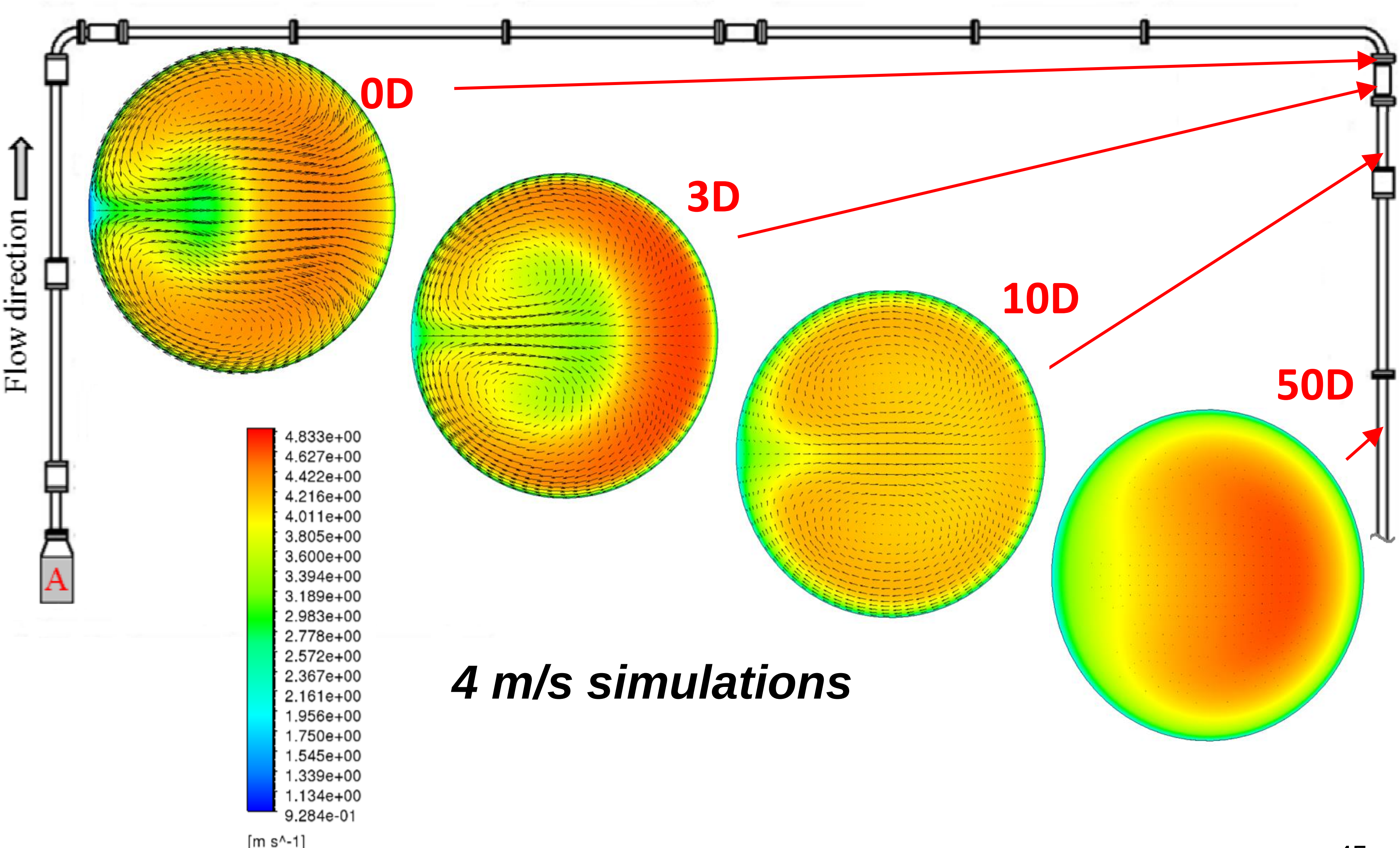

CFD models were analyzed at 0D, 3D, 10D, and 50D after the vertical-downward elbow.

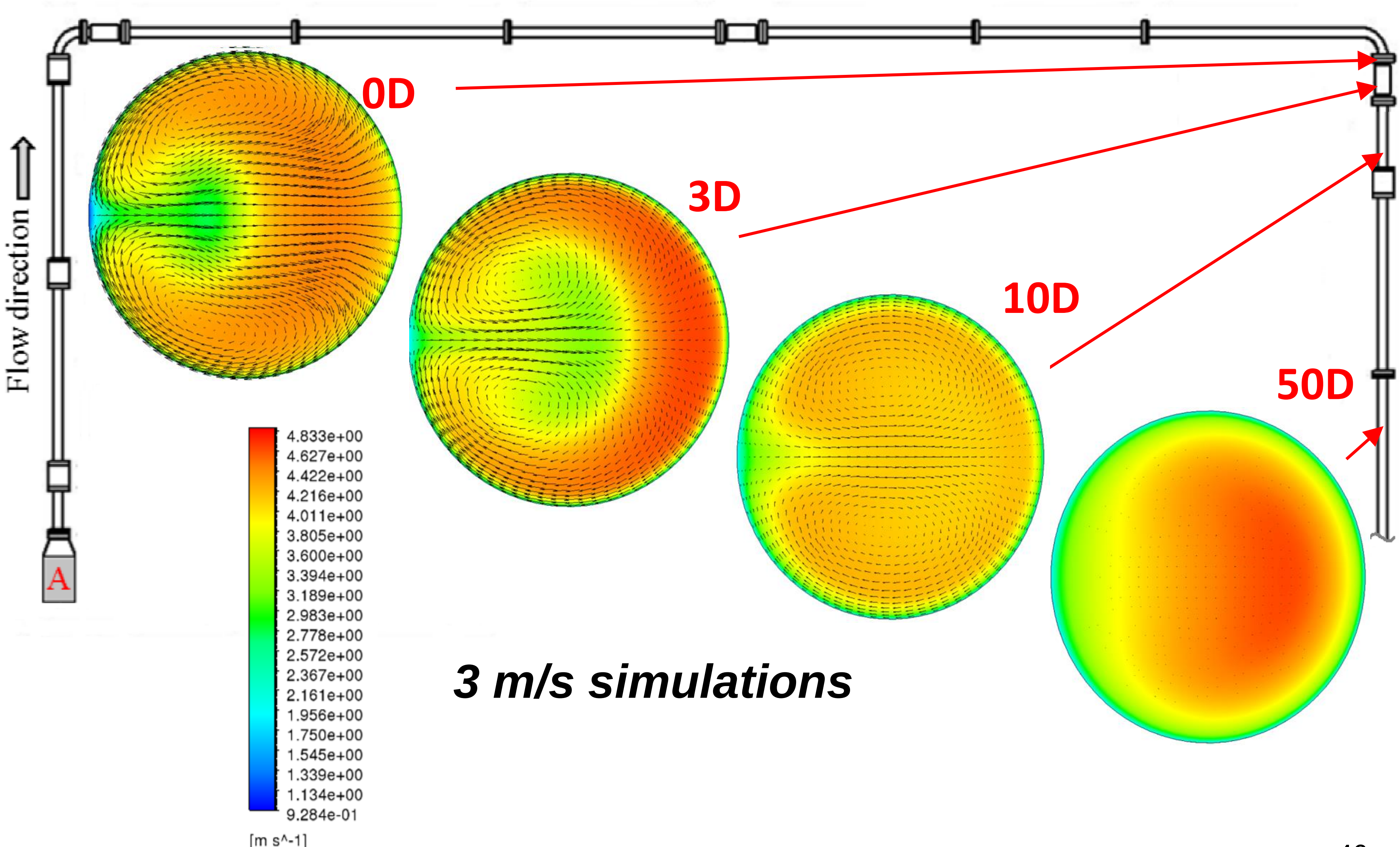

3 m/s simulations

CFD models were analyzed at 0D, 3D, 10D, and 50D after the vertical-downward elbow.

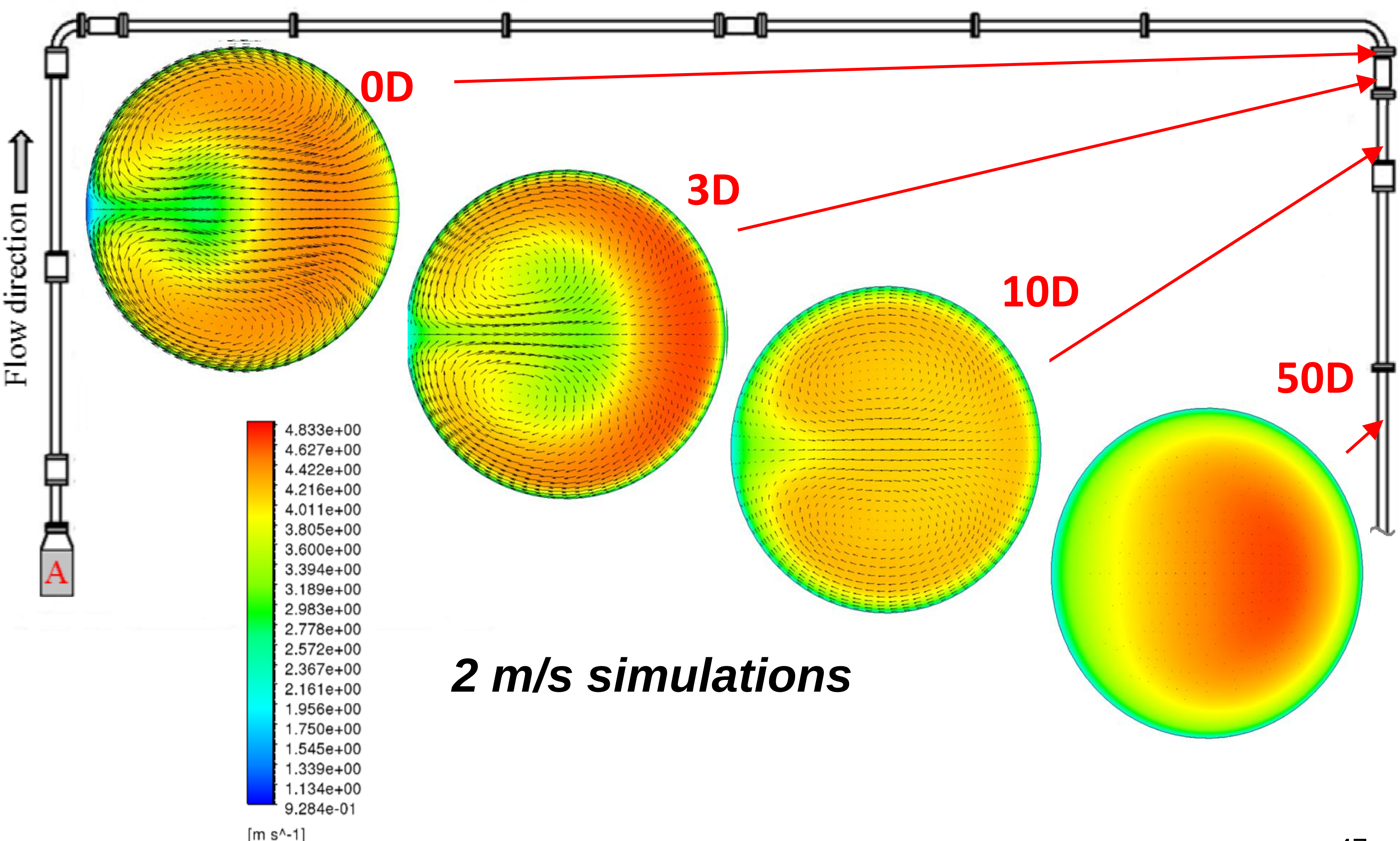

2 m/s simulations

Pressure distribution changes at 0D, 1D, and 3D after the vertical-downward elbow (4m/s)

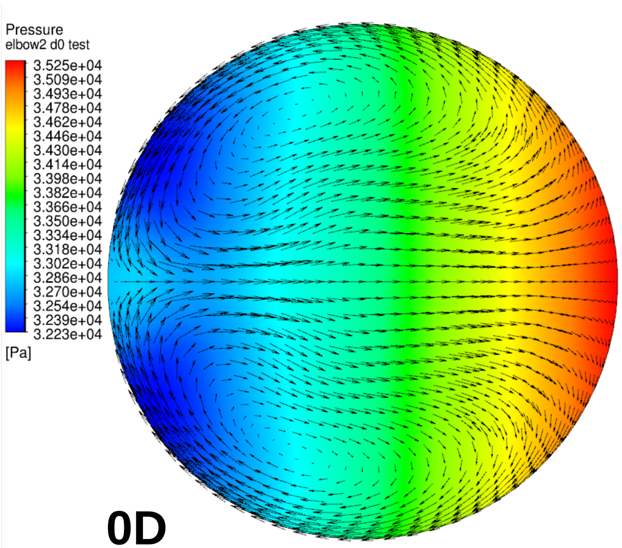

0D

8.6% absolute pressure difference

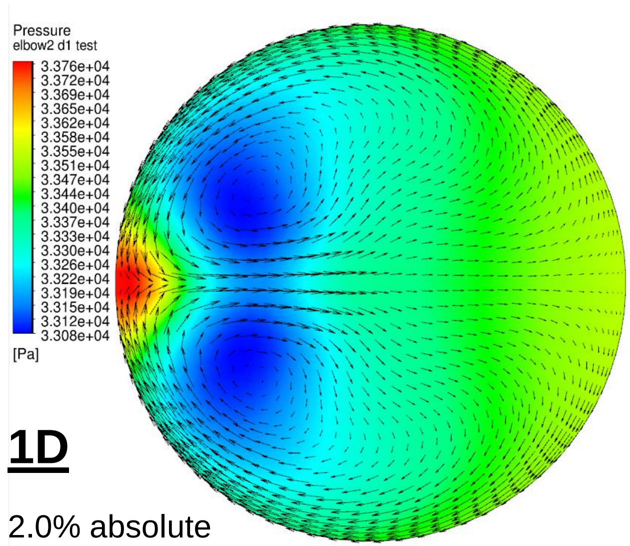

1D

2.0% absolute pressure difference

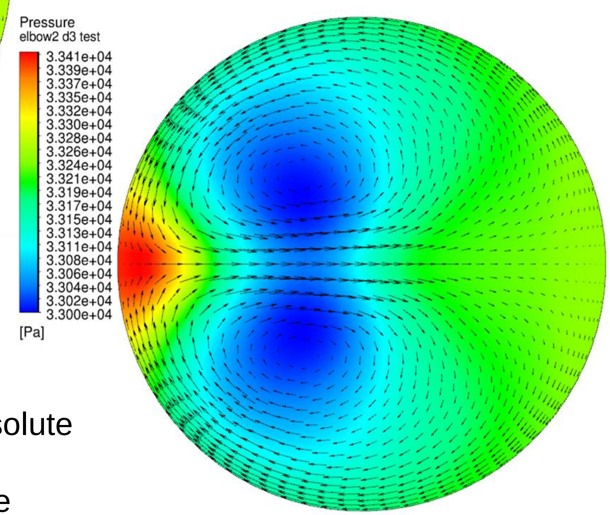

3D

1.3% absolute pressure difference

The area average void fraction and elbow strength of our data is comparable to previous research.

	Current	**Mena**	**% Difference**
RUN 7			
<α> [-]	0.047	0.066	28.8%
σ [-]	0.4821	0.5638	14.5%
RUN 5			
<α> [-]	0.031	0.034	8.82
σ [-]	0.2464	0.2422	1.73
RUN 8			
<α> [-]	0.046	0.05	8.00
σ [-]	0.2642	0.2585	2.21

The area average void fraction and elbow strength of our data is comparable to previous research.

Run 7 3D

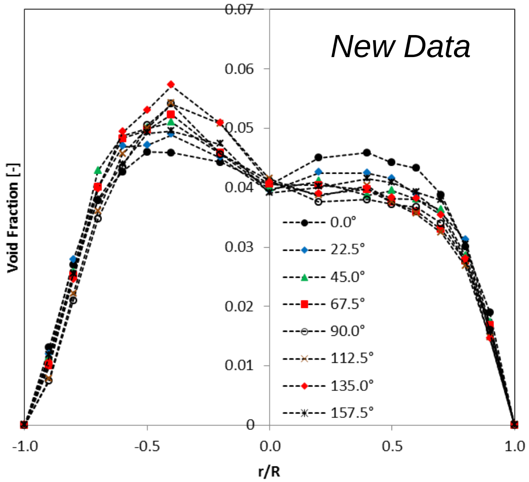

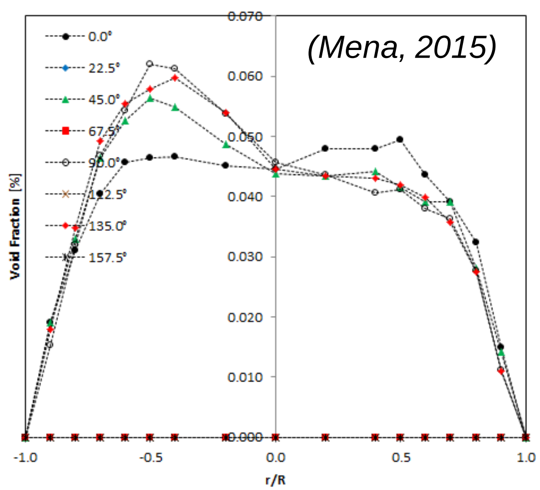

Run 8 3D

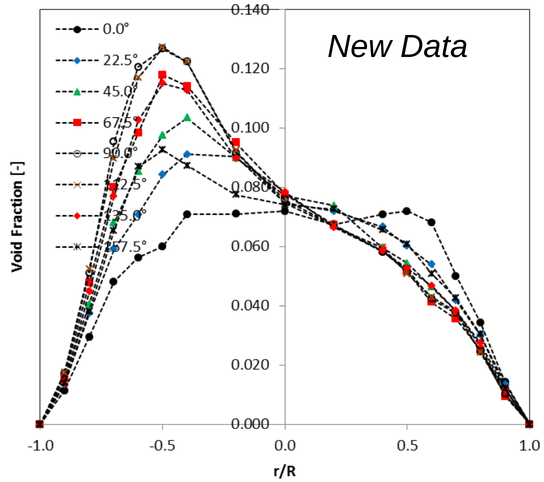

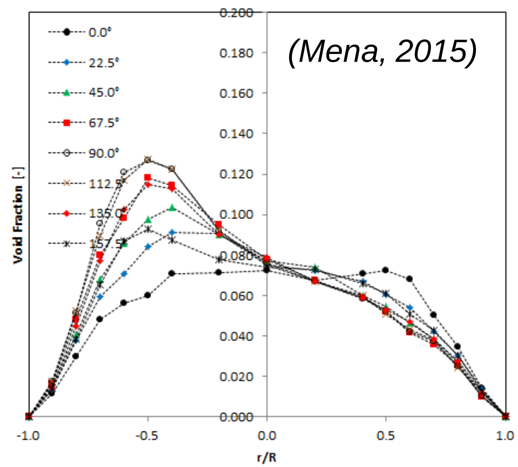

Run 5 3D

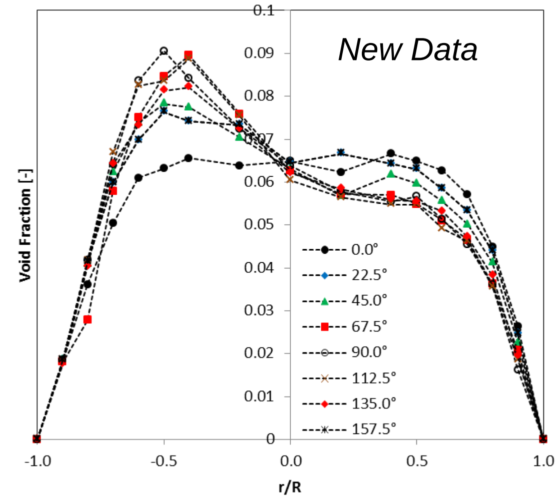

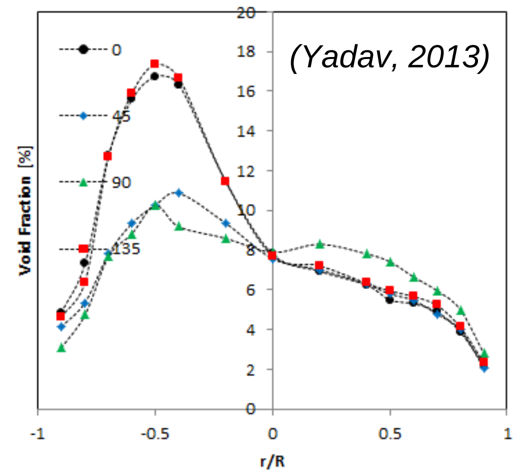

OpenFoam simulations from Kim et al. (2014) agree closely with CFX results over entire elbow length.

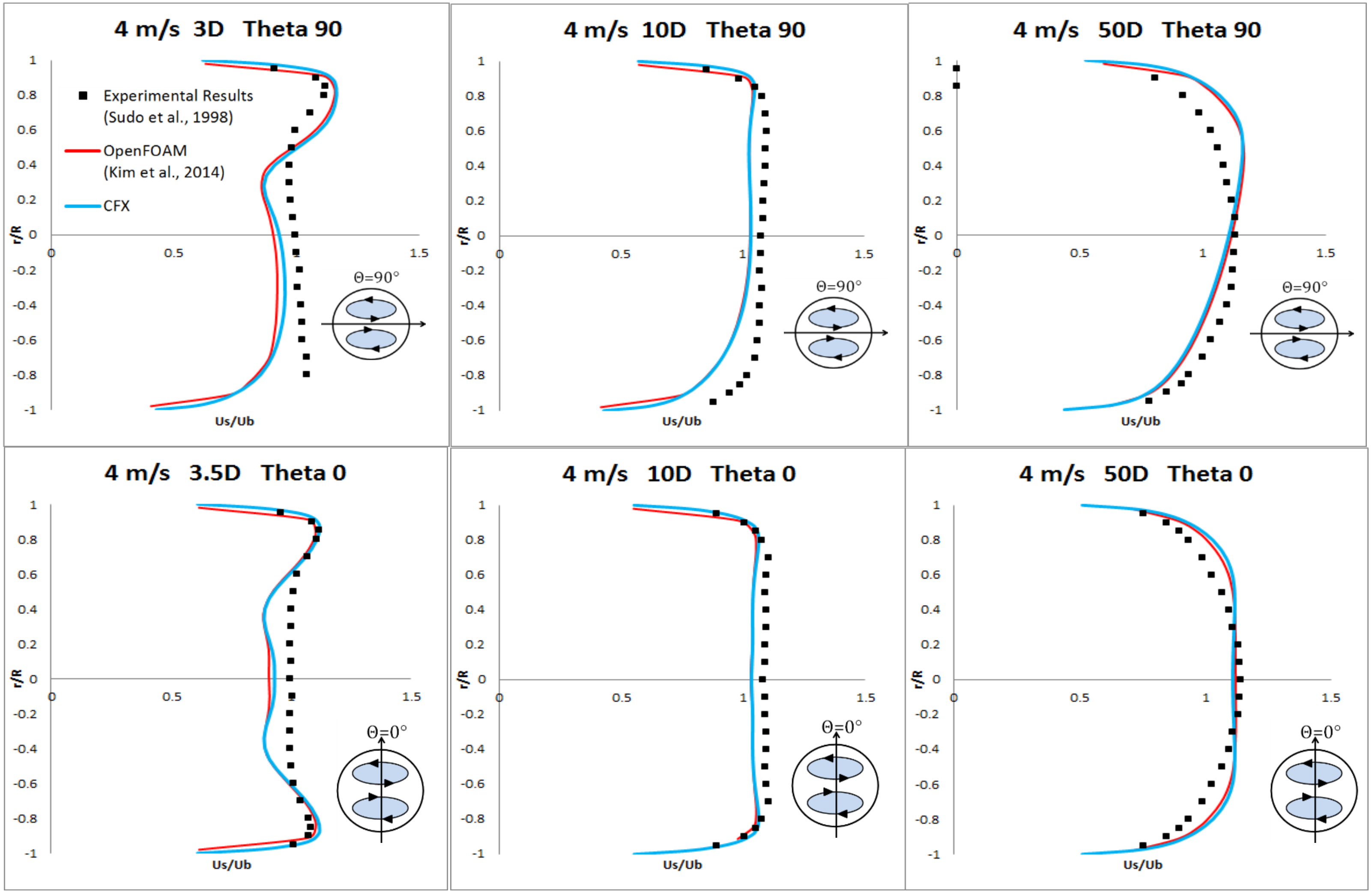

Surface contours created from previous studies help better understand flow regime of the facility

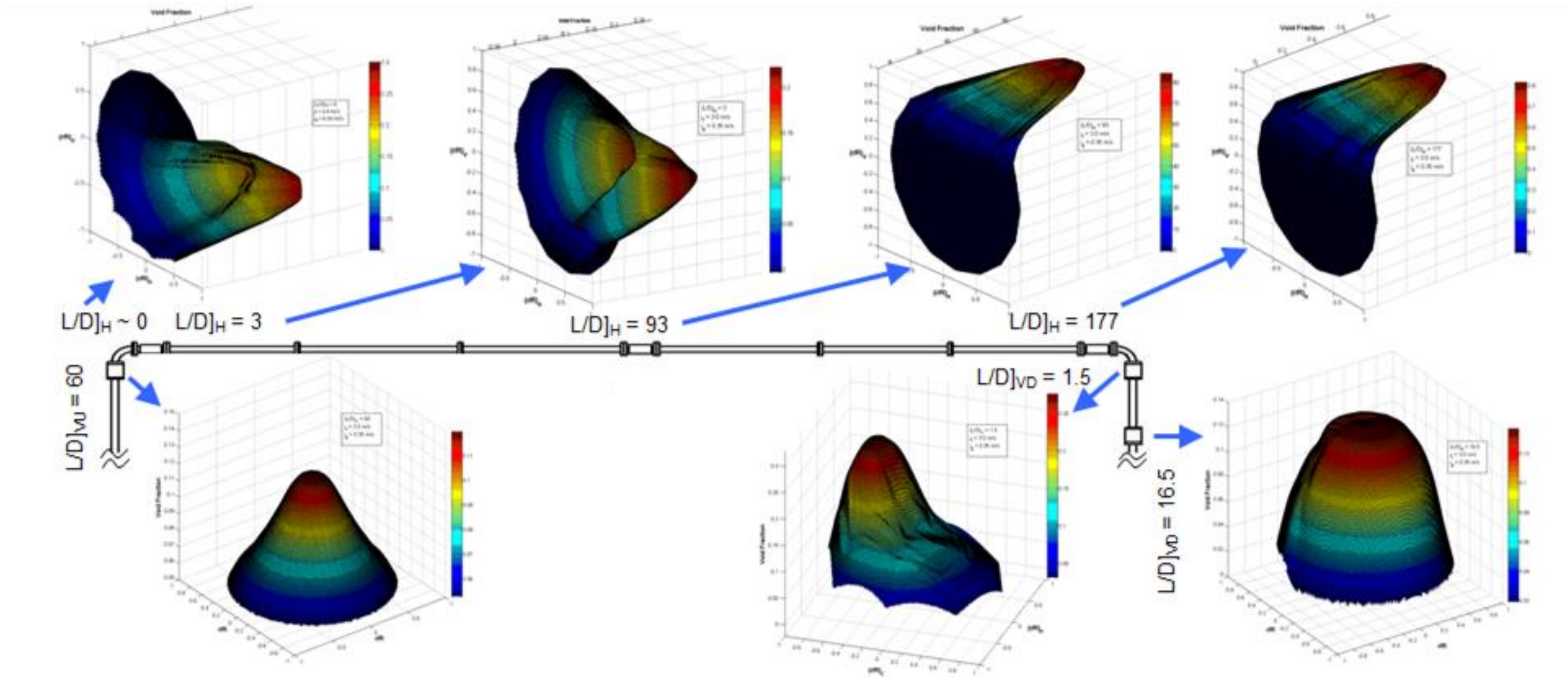

Surface plots and Contour plots show void fractions from experiments.

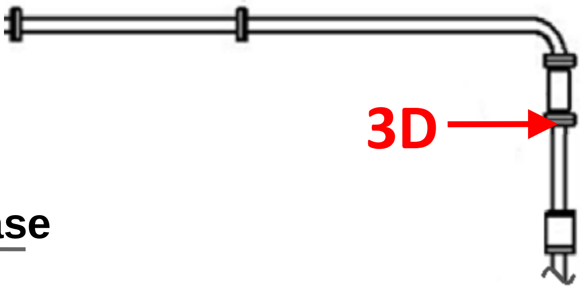

Local Void Fraction (α) = $\frac{\text{time occupied by gas phase}}{\text{total time}}$

Repeat experiments, such as Run 5, confirm consistency with previous data.

Run 5

Volumetric liquid flux: 3.00 m/s
Volumetric gas flux: 0.23 m/s

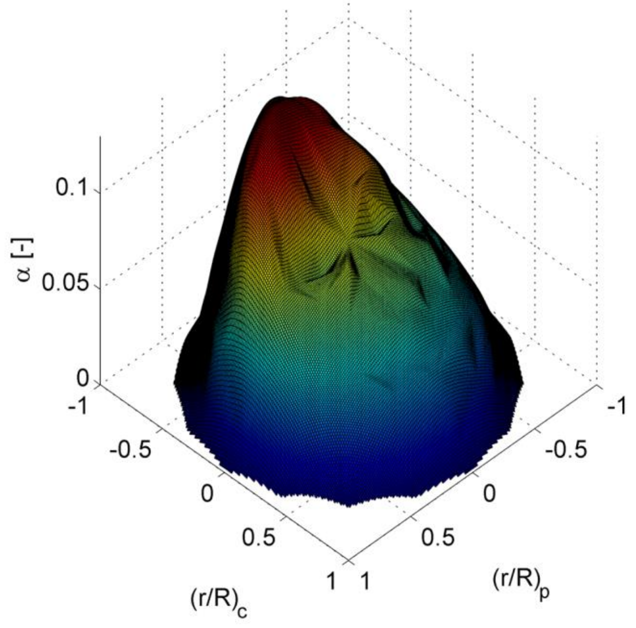

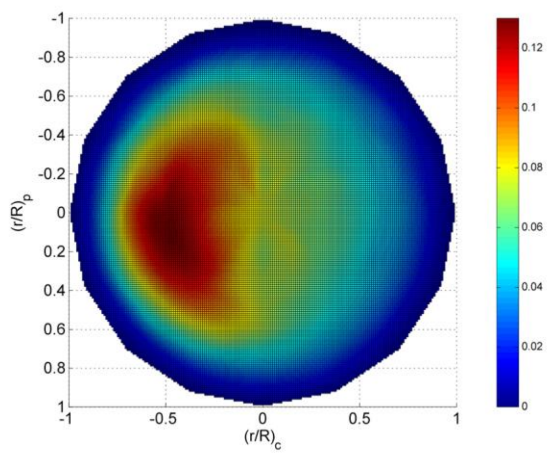

The objective of this research is to investigate two-phase flow after a vertical-downward elbow.

Bubbly Flow In Vertical Pipe

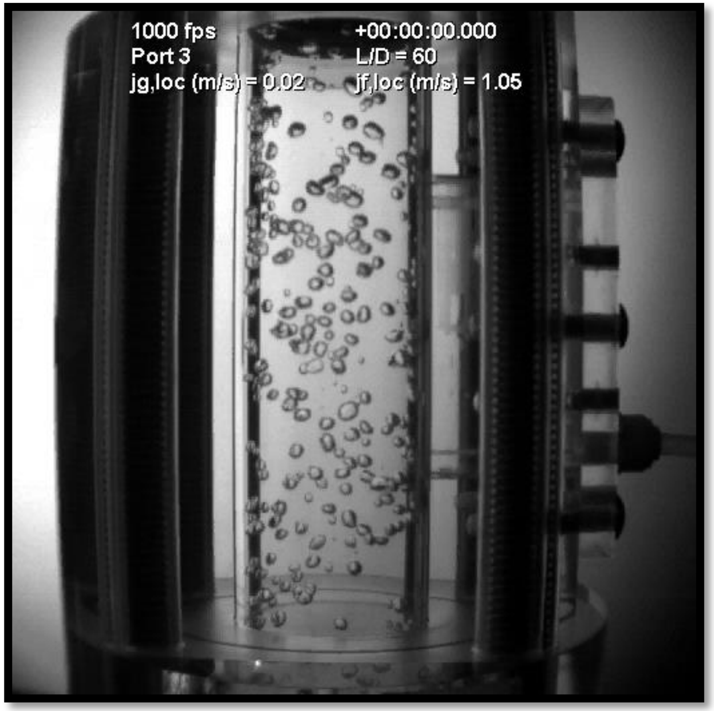

Bubbly Flow In Vertical-Upward Elbow

Flow rates and geometry dramatically change flow characteristics